THE ECONOMIC FEASIBILITY OF PUMPED STORAGE HYDROPOWER

Final Report

by Lisa Mae Dilley

Hydro Research Fellow

Washington State University

March, 2015

Academic Advisor: Michael E. Barber

ACKNOWLEDGEMENT

I would like to thank my advisor, Mike Barber, and my committee members for their assistance and encouragement in the process of preparing this research.

I would particularly like to thank my husband, Scott, and my children for their unflagging support and their willingness to embrace the adventure that my education has turned out to be for all of us.

Thank you, also, to the U.S. Department of Energy and to the Hydro Research Foundation. The information, data, or work presented herein was funded in part by the Office of Energy Efficiency and Renewable Energy (EERE), U.S. Department of Energy, under Award Number DE-EE0002668 and the Hydro Research Foundation.

DISCLAIMER

THE ECONOMIC FEASIBILITY OF PUMPED STORAGE HYDROPOWER

Abstract

by Lisa Mae Dilley

Hydro Research Fellow

Washington State University

March, 2015

Academic Advisor: Michael E. Barber

There is little general modeling research available for evaluating new PSH proposed for development from an economic point of view. This modeling framework enables the analyst to evaluate hypothetical pumped-storage within the generation fleet that it would be built in with limited data requirements on the front end. Using shortest paths optimization and a k-shortest paths technique, a simulation model is developed that demonstrates the potential effects of storage on a thermal generation system. It is shown that these simulation results reproduce analytical economic efficiency conditions, which gives specific insight to the sensitivity of PSH to design choices and wind statistics. It is shown that system marginal cost and total cost can be reduced through operations policies. These results also inform the need for additional data and detailed modeling in the feasibility stages of design.

Contents

List of Tables

List of Figures

Part I

Introduction

Pumped storage hydropower (PSH) is an integral part of the energy grid worldwide and is considered to be an important part of a grid-scale renewable energy scheme [Carrasco et al., 2006; Ibrahim et al., 2006; Levine 2003]. Developers faced with wind-balancing challenges must provide sufficent generation and energy reserves to offset the natural and unpredictable fluctuations in wind and solar energy generation. One strategy is to set aside conventional generators, which may have to operate off of their best efficiency point (BEP), to provide this reserve capacity. The drawbacks to this approach are two-fold. First, the partially loaded generators involved often experience increased fuel and maintenance costs. Second, generators can only ramp down to minimum power output. In regions with regulatory penalties for shedding wind generation when it is not needed, this minimum generation level can lead to oversupply situations. The value of demand response in addition to turning off conventional generators can be quite high during these times.

PSH is uniquely suited to solving both these drawbacks. Pump/turbines used for PSH are capable of fast ramping with a relatively wide operating range, making them suitable for balancing wind power where conventional generators may not be. During times of oversupply, pump/turbines can provide demand response, which avoids costly shutdowns of both wind turbines and conventional thermal generators. To make development of PSH feasible in sufficient quantities to complement renewable energy integration, the economics of pumped storage must be better understood, particularly for application during the feasibility stage of development. The developer must know two things about how PSH will interact with the production system. First, how does the timing and variability of wind create a need for load response or peak shaping? Second, how does PSH development affect system cost and therefore the economics of adding storage capacity?

To understand how PSH can benefit the grid, I look at the costs associated with storage in three ways. To begin with, a detailed look at the variability of intermittent power generation helps to characterize the demand conditions under which pumped storage development and operating decisions are being made. I make the first application of GARCH regression analysis to aggre-

gated wind power. I suggest using the changes in net load variance over time to better understand the role storage plays in mitigating the impact of renewable generation on the power system. Next I use the economic efficiency conditions of a system with intermittent generation and storage to develop relationships between production marginal cost and storage decisions and discuss the intertemporal relationships among demand, storage decisions, and intermittent generation. These economic calculations are the first to include intermittent generation with storage and to explicitly characterize the interaction among storage capacities, storage decisions, and costs. Finally, I use a dynamic simulation of pumped storage operations, given net load and realistic operating constraints, to more finely detail the effect of storage decisions on system cost. I use the GARCH model to implement a two-stage decision-making model based on rolling forecasts and show how a system with high variability takes advantage of PSH.

Pumped Storage Modeling

As of 2009, there were 300 PSH plants worldwide, with an installed generation capacity of 127 GW [Ingram, 2010]. Development of PSH originally occurred alongside inflexible nuclear and coal generators for the purpose of providing flexibility and peaking power. Recent interest in the development of green energy, the implementation of Renewable Portfolio Standards (RPS), and market liberalization in the United States and abroad have spurred new interest in PSH [Yang, 2011]. Europe catalogs 7400 MW of proposed PSH, 2014 MW of which is in Switzerland [Deane, 2010]. In the United States, 39 preliminary permits for PSH were filed between 2005 and 2010, for a total of 33 GW of new pumped storage [Hadjerioua et al., 2011]. Preliminary permits are not construction permits and only give the holder priority rights to a site for three years while preliminary studies are being conducted. Variability in energy supply, volatility in energy markets, and overall energy security are reasons cited by European developers for their interest in PSH [Deane, 2010; Black and Strbac, 2007]. North American developers show interest in building pumped storage to mitigate wind variability as well as for water resource purposes including water storage, in-stream flow augmentation, water treatment, and water quality mitigation [Yang, 2011; BPA, 2010; Benitez et al., 2008].

PSH studies often calculate the value of a proposed PSH development based on historical

prices and hypothetical operating policies. PSH models are typically tailored to a specific context. Pumped storage is modeled on time scales ranging from a monthly or seasonal reservoir model perspective [Liu et al., 2011; Tilmant et al., 2008; Tue et al., 2008] to hourly unit commitment models [Taylor et al., 2012; Hadjerioua et al., 2011; Olivares, 2008]. Most reservoir operations models include hedging rules that require multiple-stage decision making [Zhao et al., 2011; Tu et al., 2008]. Power operations models, which are concerned with short planning horizons, are solved on a sub-hourly timestep, as in Wang and Liu [2012].

There is a lack of general modeling of PSH. PSH models are typically studied based on regional grid assumptions [Anagnostopoulos and Papantonis, 2008; Garcia-Gonzalez et al., 2008; Bueno and Carta, 2005a, 2005b], and they focus on small scale wind/hydro coupling (see also Castronuovo and Lopes [2004]). The market context in PSH models varies. Some use statistical simulations based on historic energy prices [Wang and Liu, 2012; Garcia-Gonzalez et al., 2008; Katsaprakak et al., 2008] while others make direct use of historic energy price (Bueno and Carta 2005a, 2005b). Real options are studied by Hedman and Sheble [2006] and Reuter et al. [2012].

A few models study ancillary services pricing, under the assumption that storage is available. Ancillary services pricing is typically calculated based on power flow and unit commitment models [Lamadrid and Mount, 2012; Li and Shahidehpour, 2005; Wu et al., 2004]. In contrast, Hadjerioua et al. [2011] make direct use of historic ancillary prices.

These models typically leave out one or more vital characteristics of PSH. The uncertainty in planning and operating pumped storage and the effect PSH may have on the grid system are hinderances to developing an asset that is so capital intensive. My literature review includes a number of modeling papers, each of which focuses on specific aspects of storage. The following sections list these papers and their contributions. An effort to unify these research approaches is the logical next step in understanding the role of PSH in the energy economy.

Capacity

Ambec and Crampes [2012] studied the efficient entry of renewables into the energy market from the central planner's perspective. The model makes simplifying assumptions regarding the probability of wind generation, min/max levels of deployed generation, and pricing. The model incorpo-

rates long-term with short-term optimization and begins to address the overall generation mix, as well as implications for pricing over the long term. However, energy storage technologies are not included in the generation mix and variable energy is assumed to be stationary. The ability of PSH to provide demand response and the time-averaged operating costs of PSH are not addressed.

Sizing of PSH is also addressed using detailed optimization/simulation models of coupled wind-hydro systems. Anagnostopoulos and Papantonis [2008] and Bueno and Carta [2005a, 2005b] develop detailed models including European energy tariffs and market and wind data. This approach varies from general economic modeling by capturing real-time fluctuations in wind power output. They show how such modeling efforts can be useful for optimizing size, sensitivity experiments, and multi-objective optimization. The power systems are very specific to islanded systems and models address a vertically integrated power producer's objectives. The grid descriptions and market context make their models inapplicable to many potential storage applications.

Uncertainty

PSH has a design life of 30 years or more and a construction horizon of up to 10 years. The conditions under which a pumped storage is built today will change, and the nature of that change is unknown. Changes in regulatory constraints, market conditions, and grid conditions all affect the way the grid is operated. It is vital to understand these effects more thoroughly.

Reservoir optimization models are often considered to be multistage decisions. Either long-term rule curves or hedging rules are developed using forecasts or real-time decisions are made based on multiple simulated realizations of the stochastic processes involved. Zhao et al. [2011] describe the development of economic optimality conditions for reservoir operations under hydrologic uncertainty using hedging rules. Alternatively, Tilmant et al. [2008] describe the optimal operation of a system of reservoirs incorporating hydrologic uncertainty using a stochastic dual dynamic program, which also provides marginal benefit data on five different water allocation benefits.

Wang and Liu [2012] resolve the hydropower reservoir problem into multiple time scales to address forecasting error and then used dynamic programming to optimize hydropower reservoir operations over time. Chao [2012] modeled statistical uncertainty and defined the efficiency con-

ditions for generating and pricing power. None of these models includes energy storage as an economic function.

Variability

Closely related to the issue of uncertainty is variability. Variability is the stochastic fluctuations in power generated by intermittent power resources, such as wind power. The way that intermittent energy production has affected grid operations and the need for reserves is under investigation. Lamadrid and Mount [2012] examine ramping costs, and Wu et al. [2004] calculate ancillary services prices using optimal flow models. Taylor et al. [2012] use inventory control modeling to approach the same result. Even when simplified, these models are quite complex, both theoretically and computationally. Their results must be interpreted in the appropriate market context and simplified for the purpose of making investment planning decisions.

In Strbac et al. [2007] and Black and Strbac [2007] the relative size of installed wind to installed storage capacity was examined for the case of Great Britain using an hourly time step simulation model. Methods for efficiently simulating the wind/demand time series were developed in Sturt and Strbac [2011a, 2011b]. Their analysis is narrow in application and should be examined for usefulness in a larger grid context.

Economic Viability

The majority of models used in economics and engineering are profit maximization models over a given period. Hadjerioua et al. [2011] modeled the profit potential of two PSH facilities for Oak Ridge National Lab (ORNL), based on energy arbitrage, peaking, and reserve capacity. This conveniently transparent model includes reserve capacity on a relatively small, hourly time step. However, the model was entirely deterministic, having been based on one year of actual prices in specific markets. The authors note that the results are the upper bound on potential profit. They also suggest the actual market prices need to be revisited because they were established based on the marginal development cost of new thermal energy, which is significantly cheaper than new energy storage. Similar models are developed as operations models, utilizing sub-hourly time steps and complex wind forecasts (e.g., Wang and Liu, [2012]). Such operations models do

not take a long view toward investment but by reducing some of the computational complexity could be adapted to long-term analysis. Any such model will need to include stochastic price and demand inputs and, as suggested by the ORNL analysis [Hadjerioua et al., 2011], be adapted to endogenously determined ancillary services prices.

Economist Pindyck [2002] and colleague Balikcioglu [2011] solve the profit optimization problem to determine the timing and level of resource allocations, a model with relevance to PSH investment and planning. Horsley and Wrobel [2002] develop a profit-maximization model to value the energy storage potential of pumped storage, which they view as a simplified version of conventional hydropower. Horsley and Wrobel [2007] expand the model to include hydrologic inputs. Taylor et al. [2008] also assign an economic value to the stored water, using their inventory-control approach to maximize profit. These models approach the question of *how much storage and when* but need to be adapted to the market conditions of interest.

Goals and Objectives

The overall goal of this research is to develop a generic pumped storage operations model that provides insight into optimal design choices which can be used for improved evaluation of PSH projects during the planning phase. The objectives required to complete this research goal are the following:

1. Model net load using GARCH in a way that preserves heteroscedasticity and nonstationarity for use in planning models.

2. Demonstrate the effect of PSH on system cost, using the GARCH model for net load and the unit commitment model for capacity decisions.

This paper is unique because of its effort to challenge fundamental assumptions that are made regarding pumped storage hydropower, namely that the value of PSH is based only upon energy arbitrage and that the conditions under which that value is derived are stationary.

This new model achieves these innovations:

- The model explicitly calculates the time-dependent parameterization of wind/load profiles in a novel way using a GARCH model rather than adaptations of autoregressive and autore-

gressive moving average models. Periodicity of both variance in innovations and mean net load are preserved by the GARCH model and it is successfully applied to the simulation in Part IV.

- The cost-minimization model provides an estimate as to how changing market conditions affect the value of a PSH project by developing analytical expressions rather than numerical simulations for the value of energy storage.

I show that the interaction between general grid-level parameters - particularly the availability of intermediate thermal generation - are sensitive to increasing variability on the net load profile. The optimal pump/storage cycle length is dependent on the relative installed wind capacity and the temporal wind distribution. A given pumped storage reservoir capacity can serve a range of wind generation balancing needs with a 5-10% potential decrease in system variable costs.

The rest of this dissertation is organized as three separate manuscripts in preparation for submission to the appropriate journal. Part II is a detailed analyis of the statistics of net load in BPA. Part III is a detailed report on the economic calculations that incorporate net load data from Part II and inform storage design decisions that could be utilized in a detailed unit commitment model or engineering design.

Works Cited

Ambec, S., and C. Crampes (2012), Electricity provision with intermittent sources of energy, Resource and Energy Economics, 34(3), 319–336, doi:10.1016/j.reseneeco.2012.01.001.

Anagnostopoulos, J. S., and D. E. Papantonis (2008), Simulation and size optimization of a pumped–storage power plant for the recovery of wind-farms rejected energy, Renewable Energy, 33(7), 1685–1694, doi:10.1016/j.renene.2007.08.001.

Balikcioglu, M., P. Fackler, and R. Pindyck (2011), Solving optimal timing problems in environmental economics, Resource and Energy Economics, 33(3), 761–768.

Benitez, L. E., P. C. Benitez, and G. C. van Kooten (2008), The economics of wind power with energy storage, Energy Economics, 30(4), 1973–1989, doi:10.1016/j.eneco.2007.01.017.

Berry, T., and M. Jaccard (2001), The renewable portfolio standard, Energy Policy, 29(4), 263–277, doi:10.1016/S0301-4215(00)00126-9.

Black, M., and G. Strbac (2007), Value of Bulk Energy Storage for Managing Wind Power Fluctuations, IEEE Transactions on Energy Conversion, 22(1), 197 –205, doi:10.1109/TEC.2006.889619.

Bueno, C., and J. A. Carta (2005a), Technical–economic analysis of wind-powered pumped hydrostorage systems. Part II: model application to the island of El Hierro, Solar Energy, 78(3), 396–405.

Bueno, C., and J. A. Carta (2005b), Technical–economic analysis of wind-powered pumped hydrostorage systems. Part I: model development, Solar Energy, 78(3), 382–395.

Carrasco, J. M., L. G. Franquelo, J. T. Bialasiewicz, E. Galvan, R. C. PortilloGuisado, M. A. M. Prats, J. I. Leon, and N. Moreno-Alfonso (2006), Power-Electronic Systems for the Grid Integration of Renewable Energy Sources: A Survey, IEEE Transactions on Industrial Electronics, 53(4), 1002–1016, doi:10.1109/TIE.2006.878356.

Castronuovo, E. D., and J. A. P. Lopes (2004), Optimal operation and hydro storage sizing of a wind–hydro power plant, International Journal of Electrical Power & Energy Systems, 26(10), 771–778, doi:10.1016/j.ijepes.2004.08.002. Deane, J. P., B. P. Ó Gallachóir, and E. J. McKeogh (2010),

Techno-economic review of existing and new pumped hydro energy storage plant, Renewable and Sustainable Energy Reviews, 14(4), 1293–1302, doi:10.1016/j.rser.2009.11.015.

Eyer, J., and G. Corey (2010), Energy storage for the electricity grid: Benefits and market potential assessment guide, Sandia National Laboratories Report, SAND2010-0815, Albuquerque, New Mexico.

Garcia-Gonzalez, J., R. M. R. de la Muela, L. M. Santos, and A. M. González (2008), Stochastic joint optimization of wind generation and pumped-storage units in an electricity market, Power Systems, IEEE Transactions on, 23(2), 460–468.

GE Energy (2010), Western Wind and Solar Integration Study

Goodenough, J. B., H. D. Abruna, and M. V. Buchanan (2007), Basic research needs for electrical energy storage, in Report of the basic energy sciences workshop for electrical energy storage, vol. 186.

Hedman, K. W., and G. B. Sheble (2006), Comparing Hedging Methods for Wind Power: Using Pumped Storage Hydro Units vs. Options Purchasing, in International Conference on Probabilistic Methods Applied to Power Systems, 2006. PMAPS 2006, pp. 1–6.

Horsley, A., and A. J. Wrobel (2002), Efficiency rents of pumped-storage plants and their uses for operation and investment decisions, Journal of economic dynamics and control, 27(1), 109–142.

Horsley, A., and A. J. Wrobel (2007), Profit-maximizing operation and valuation of hydroelectric plant: A new solution to the Koopmans problem, Journal of Economic Dynamics and Control, 31(3), 938–970. Ingram, E. (2010), Worldwide Pumped Storage Activity, Renewable Energy World.

Lamadrid, A. J., and T. Mount (2012), Ancillary services in systems with high penetrations of renewable energy sources, the case of ramping, Energy Economics, 34(6), 1959–1971, doi:10.1016/j.eneco.2012.08.011.

Li, T., and M. Shahidehpour (2005), Price-based unit commitment: a case of Lagrangian relaxation versus mixed integer programming, IEEE Transactions on Power Systems, 20(4), 2015–2025, doi:10.1109/TPWRS.2005.857391.

Liu, H., E. Erdem, and J. Shi (2011), Comprehensive evaluation of ARMA–GARCH (-M) approaches for modeling the mean and volatility of wind speed, Applied Energy, 88(3), 724–732. Pindyck, R. S. (2002), Optimal timing problems in environmental economics, Journal of Economic Dynamics and Control, 26(9), 1677–1697.

Reuter, W. H., S. Fuss, J. Szolgayová, and M. Obersteiner (2012), Investment in wind power and pumped storage in a real options model, Renewable and Sustainable Energy Reviews, 16(4), 2242–2248.

Sioshansi, R., P. Denholm, and T. Jenkin (2012), Market and Policy Barriers to Deployment of Energy Storage, Economics of Energy and Environmental Policy, 1(2), doi:http://dx.doi.org/10.5547/2160-5890.1.2.4.

Steffen, B. (2012), Prospects for pumped-hydro storage in Germany, Energy Policy, 45, 420–429, doi:10.1016/j.enpol.2012.02.052.

Strbac, G., Shakoor, Anser, M. Black, D. Pudjianto, and Thomas Bopp (2007), Impact of wind generation on the operation and development of the UK electricty systems, Electric Power Systems Research, 77(9), 1214–1227, doi:10.1016/j.epsr.2006.09.014.

Sturt, A., and G. Strbac (2011a), A times series model for the aggregate GB wind output circa 2030, in IET Conference on Renewable Power Generation (RPG 2011), pp. 1–6.

Sturt, A., and G. Strbac (2011b), Time series modelling of power output for large-scale wind fleets, Wind Energy, 14(8), 953–966, doi:10.1002/we.459. Tilmant, A., D. Pinte, and Q. Goor (2008), Assessing marginal water values in multipurpose multireservoir systems via stochastic programming, Water Resources Research, 44(12), W12431.

Wang, J., and S. Liu (2012), Quarter-Hourly Operation of Hydropower Reservoirs with Pumped Storage Plants, Journal of Water Resources Planning and Management, 138(1), 13–23, doi:10.1061/(ASCE)WR.1943-5452.0000143.

Wu, T., M. Rothleder, Z. Alaywan, and A. D. Papalexopoulos (2004), Pricing energy and ancillary services in integrated market systems by an optimal power flow, Power Systems, IEEE Transactions on, 19(1), 339–347.

Zhao, J., X. Cai, and Z. Wang (2011), Optimality conditions for a two-stage reservoir operation problem, Water Resources Research, 47(8), doi:10.1029/2010WR009971.

Part II

ARMA-GARCH Model to Characterize Aggregate Wind Power

With wind generation levels increasing around the world, energy producers and researchers are developing methodologies of forecasting wind power and integrating wind generation into the electricity generation system [Foley et al., 2012; Wang et al., 2011; Hodge and Milligan, 2011; Soman et al., 2010]. The economics of sustainable wind power production require better wind power forecasts for wind and reserve generation scheduling. Wind forecasting research highlights the need for realistic time series of wind power for dynamic simulation models and analytic stochastic process models. Energy and generation reserves for the mitigation of wind variability are allocated in various ways based on the standard deviation of wind production, historical forecast error, and net-load quantiles [Holttinen et al., 2013; Mauch et al., 2013; Ela et al., 2010; Black and Strbac, 2007]. Thus, in generation and reserve scheduling, it is important to be able to model information about not only the mean but the variability in wind power caused by wind turbulence. The generalized autoregressive conditional heteroscedasticity (GARCH) model presented in this paper describes the statistics of net load in a way that enables the simulation of historic timeseries for Monte Carlo simulations or quantile-based forward decision making. This work represents the first time wind power has been modeled with an autoregressive moving average (ARMA) mean process with GARCH innovations.

The importance of wind power statistics to system operations has resulted in an extensive body of research on the statistics of wind speed and direction as in input to wind power models. It is widely recognized in literature that wind processes are both non-stationary and heteroscedastic although the attempts to produce ensemble systems are often biased and uncalibrated [Thorarindottir and Gneiting, 2010]. Approaches have varied considerably as researchers attempt to account for local conditions. Models for wind speed have been developed based on autoregressive (AR) and autoregressive moving average (ARMA) models, Markov switching models, spectral methods, and neurological methods [Ailliot and Monbet 2012; Pinson and Madsen 2012; Sturt and Strbac 2011b; Lei et al., 2009; and Sfetsos 2000]. Because of the non-stationarity of wind patterns, the linear models such as AR must be adapted to successfully model the turbulence or heteroscedasticity of wind speed. Huang and Chulabi [1995] fitted their AR wind speed model with time-varying parameters, effectively modeling heteroscedasticity by allowing the parameterization of the mean process itself to be time-varying.

The time dependence of the variance in stochastic wind speed processes continues to be

problematic for linear models with stationary variance processes, so GARCH models have been studied widely for modeling wind speeds for the purpose of directly modeling heteroscedasticity by means of the residual series. Tol [1997] proposed a gamma GARCH model to simulate daily wind speed near Shearwater, Canada. Liu et al. [2011] examined 10 GARCH model structures on 7 years of hourly data from a Colorado site, concluding that no one model was superior for modeling wind speeds at all heights tested. GARCH models generally outperform other statistical wind models in terms of ease of implementation and simulating the periods of calm and high volatility that characterize wind speeds [Liu et al., 2012; Jeon and Taylor, 2012; Jiang et al., 2012; Tan, 2010].

However, wind speed models must be transformed by complex functions, which are often stochastic themselves, to be used in power simulations. Thus, linear regression models of wind power are tested in Chen et al. [2010] and Sturt and Strbac [2011a, 2011b]. The time-varying parameters are dealt with by fitting models seasonally (by hour of the day, month, or season of the year). Lau and McSharry [2010] modeled the the changing variance in wind power directly using an ARMA-GARCH model fitted to wind power data transformed to follow the normal distribution. Trombe et al. [2012] adapted a Markov switching wind power model with GARCH innovations for simulation of wind variability on a very short time scales.

The objective of this chapter is to develop a GARCH wind power model that preserves heteroscedasticity and nonstationarity for hourly simulation useful for long-term operations simulations. The wind power data for BPA are here aggregated with total load to create a historical net-load timeseries over the entire period of operation of the BPA wind fleet. The variability of the resulting load curve is modeled using an asymmetric GARCH model. The economic model in Part III uses the simulated net load statistics to calculate optimal storage capacity investments and deployments, and the model developed in this chapter is used in Part IV to simulate net load scenarios to be used in a stochastic unit commitment simulation.

GARCH Models - Model selection

Data Introduction

BPA Balancing Authority (BPA) manages the generation and transmission needs over a region that includes the states of Washington, Oregon, Idaho, and portions of five other states. It is the responsibility of BPA to schedule and dispatch both generation and transmission to meet electricty demand within the balancing area along with scheduled energy exports. The amount of wind generation included in the generation fleet within the balancing area has increased from 250 MW in 2005 to 4515 MW in 2013 [BPA Wind, 2013], and has resulted in a number of challenges, including oversupply conditions when high wind conditions coincide with peak runoff conditions that force the hydropower system to its maximum output [BPA, 2013]. The data used for this model is historical five-minute average power generation and load data for the period 2007 through the present made available by BPA at BPA Wind [2013].

Wind power is described as “must take” energy based on regulatory constraints, and while it is schedulable within a margin of error in the short term, it is neither predictable nor dispatchable like conventional generation. Thus, wind generation is not a decision in a unit commitment problem, but more of an input in the same way that load is an input. Given this generalization, wind generation and system load are aggregated into a net load time series, defined to be $load - wind\ generation$. The resulting time series exhibits some of the noisiness of wind power, which is largely random and only very loosely correlated with time of day, while retaining the general periodicity of electricity demand. (See Figure 1.)

The proposed net load model employs a type of GARCH model, which was first developed first by Engle [1982] and generalized by Bollerslev [1986] to describe financial markets. The motivation for developing GARCH was the observation that certain financial market events created periods of volatility - clusters of large changes interspersed with periods of relatively small changes. Standard regression models like autoregressive (AR) or autoregressive moving-average (ARMA) models can be fitted to timeseries data and the stochastic innovations or residuals are modeled as a white noise process, which is serially uncorrelated. However, as in the case of financial timeseries, the residuals of a GARCH process are correlated because large changes in returns tend to follow large changes in returns. Bauwens et al. [2012] describes the autocorrelation coefficients of the

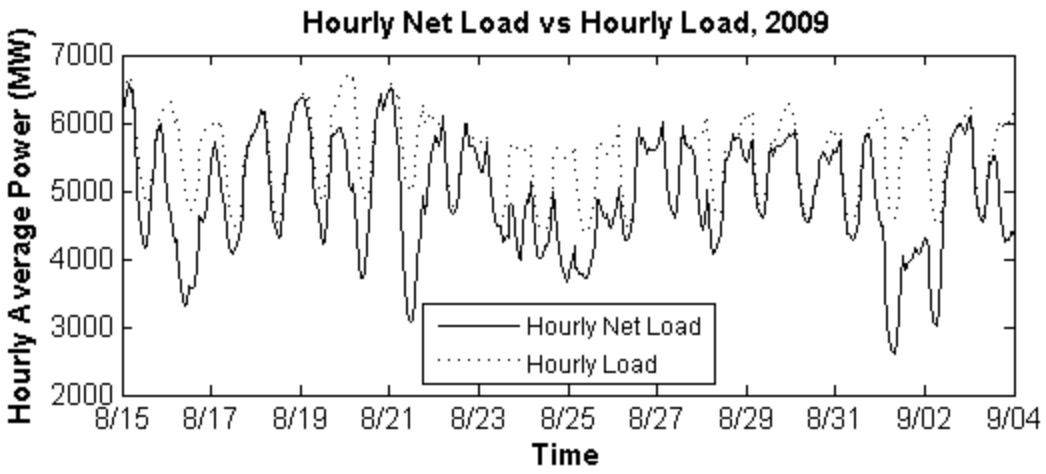

Figure 1: Net Load exhibits the periodicity of daily load while absorbing the irregular patterns of wind power generation.

squared residuals of a GARCH process as starting at a relatively small value of approximately 0.2 and slowly decreasing at increasing lags (see Figure 2). As a consequence of this correlation, the distribution of financial returns tends to be leptokurtotic - that is, the distribution of financial returns tends to have heavier tails and more mass at center than the normal distribution.

Net power demand (net load) is influenced by processes that are localized in time that create volatility clusters similar in structure to those found in financial markets. Of primary importance are meteorological processes such as sunrise and sunset, weather fronts, and storm systems. These micro processes create periods of higher winds and greater wind turbulence interspersed with periods of relative calm. Additional volatility is introduced into the wind power time series by the fact that wind turbines have physical cut-off speeds. During periods of high wind speeds, this cut-off speed may be exceeded. The turbine has safety mechanisms that disengage the generator and reduce its power output from maximum to zero when cut-off speed is exceeded. As a result, the distribution of net load data is skewed and leptokurtotic, suggesting the appropriate application of GARCH models to the data (Figure 3).

Aggregating the fleet of wind turbines with power demand has a smoothing effect on wind volatility so that minute-to-minute fluctuations have less impact on net demand and thus operating decisions, which approximates the reality of a grid-scale balancing procedure. In real-time, minute-to-minute balancing decisions are automated and operate on energy reserves set aside for that purpose. For the purposes of a long-term planning model, hourly variability is sufficient to describe

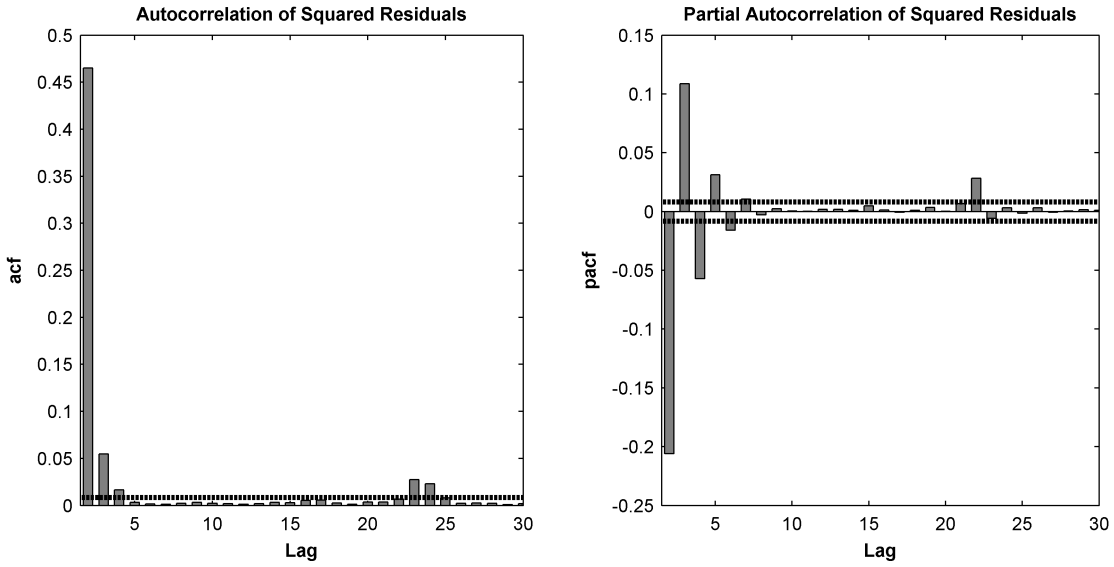

Figure 2: The residuals of the net load data are correlated to at least four lags, suggesting the appropriate application of GARCH innovations. The data modeled here are the squared residuals of the entire (non-seasonalized) net load time series modeled as an ARMA(24,1) process.

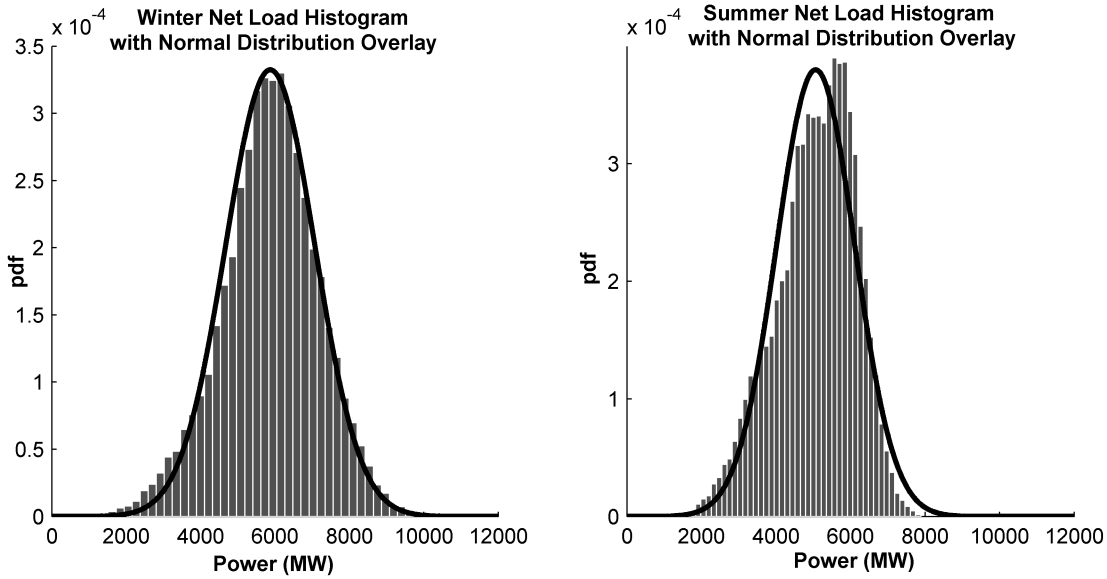

Figure 3: Both summer and winter net load values are skewed to the right compared to the normal distribution and exhibit slightly heavier left tails, and summer and winter are decidedly different from each other. (The normal curve in this case is overlayed for general reference and is only linked to the data in that the mean of the reference curve is equal to the sample mean.)

the operating potential of a proposed facility.

GARCH Models - General

The model used to fit the net load time series consists of a parametric mean process with a GARCH process for the series residuals. A typical GARCH model can be expressed as

$$y_t - \mu_t = \varepsilon_t = \sigma_t z_t \tag{1}$$

where t represents the current timestep, y_t is the series value, ε_t is the series innovation, μ_t is the conditional series mean at time t, σ_t is the square root of the conditional variance of the series, and the series $\{z_i\}$ is independently and identically distributed (i.i.d.) on a standardized conditional distribution. The mean process is commonly specifed as an ARMA model with general form

$$y_t = \mu + \sum_{i=1}^{p} \phi_i y_{t-i} + \sum_{j=1}^{q} \theta_j \varepsilon_{t-j} + \varepsilon_t \tag{2}$$

where p is the AR order (the number of lagged series value terms), q is the moving average (MA) order (the number of lagged error terms), μ is a constant, ϕ and θ are the AR and MA coefficients respectively, and i and j are the lag values. The number of lags taken into account are selected during model specification, and an ARMA model with p AR terms and q MA terms is specified as ARMA(p,q). When $p = 0$, the model reduces to a moving average model, MA(q), and when $q = 0$ the model reduces to an AR(p) model. The order of the mean process is selected with guidance from the autocorrelation and partial autocorrelation functions as described below.

Instead of specifying a white noise process for the innovations ε_t in equation 2, GARCH models allow ε_t to have a changing variance with time such that $\varepsilon_t = \sigma_t z_t$. σ_t^2 is thus the conditional variance of the process. Volatility is the descriptive term of this conditional variance. σ_t^2 is conditioned on the square of the error terms, ε_t, and the variances, σ_t^2, of previous time steps. The GARCH model is then specified as a parametric regression model, the most common of which is standard GARCH, denoted sGARCH(k,l):

$$\sigma_t^2 = (\omega + \sum_{j=1}^{m} \zeta_j v_{jt}) + \sum_{i=1}^{k} \phi_i \sigma_{t-i}^2 + \sum_{j=1}^{l} \theta_i \varepsilon_{t-j}^2 \tag{3}$$

where ω, ϕ_i, θ_i are constants, σ^2_{t-k} is the conditional variance observed k timesteps back, and ε_{t-j} is the residual observed j timesteps back. In the sGARCH specification, the constants are constrained such that $\mu_0 > 0$, $\phi_i \geq 0$, $\theta_i \geq 0$ [Bauwens et al., 2012]. The persistence of the model, $P = \sum_i \phi_i + \sum_j \theta_j$, describes how far into the future conditional variance at time t continues to have influence on conditional variance. GARCH volatility typically dies off exponentially, with a exponent value $P < 1$. If $P = 1$, the influence of conditional variance does not die off and persists to $t = \infty$, causing the variance to blow up. To ensure stationarity, $P < 1$. When the persistence of a GARCH model is nearly 1, additional explanatory data is often useful. When available, this additional data can be regressed on the GARCH equation where ζ_j are the regression parameters and v_{jt} are the data points.

sGARCH is a linear combination of previous error terms and conditional variances, but in some processes the non-linear components are significant. Non-linear GARCH models include non-linear GARCH (NGARCH), quadratic GARCH (QGARCH), and Glosten-Jagannathan-Runkle GARCH (GJRGARCH). A brief description of these models is included in the Appendix A. but they are not discussed in detail here.

The constraints on the constants in the sGARCH formulation ensure that the resulting distribution of residuals is symmetric. However, many series are not symmetric, and there are two mathematical sources of asymmetry. In the first case, when the autocorrelation of the residuals is not symmetric, the conditional variance depends on both the size and sign of the previous previous. Asymmetric GARCH models include terms that account for sign effects, including NGARCH, QGARCH and GJRGARCH. Exponential GARCH (eGARCH) was developed by Nelson [1991] specifically citing the restrictions on sGARCH parameters as being too restrictive. In addition to sign effects, the eGARCH γ term is considered to represent the presence of leverage in the data, or the size effect, which is the presence of large changes following large changes, and conversely, small changes following small changes. eGARCH is commonly used for asymmetric processes and was shown by Liu et al. [2011] to work quite well for wind speeds. Since the net load data seems to exhibit assymetry and visually exhibits clusters of high volatility followed by clusters of low volatility, eGARCH was chosen to test against sGARCH. The formal definition of an eGARCH(k,l) process is

	ARMA	GARCH	
Regression Intercept	μ	ω	intercept constant
Regression Parameters	ϕ_i, ar_i - AR terms	α_i	ARCH terms (ε^2_{t-i}) for sGARCH
		α_i	sign parameter (z_{t-i}) for eGARCH
	θ_i, ma_i- MA terms	β_i	GARCH terms (σ^2_{t-i})
		γ_i	eGARCH size parameter
External Regressor Parameters		ζ_i	vxreg - external variance regressors
Conditional Distribution		ξ	skew
		ν	shape

Table 1: GARCH parameters as implemented in R package `rugarch`.

$$log_e(\sigma_t^2) = (\omega + \sum_{j=1}^{m} \zeta_j v_{jt}) + \sum_{i=1}^{k} \beta_i log(\sigma_{t-i}^2) + \sum_{j=1}^{l} (\alpha_j z_{t-j} + \gamma_j [|z_{t-j}| - E|z_{t-j}|]), \tag{4}$$

$$z_t = \frac{\varepsilon_t}{\sqrt{\sigma^2}}, \tag{5}$$

where E is the expectation operator. Unlike sGARCH, there is no sign restriction on the constants α_j and β_j. α_j is the constant that captures the sign effect and γ_j captures the size effect. Persistence here is defined as $P = \sum_j \beta_j$ and must be less than one for stationarity [Ghalanos, 2013].

The second source of asymmetry is the distribution of the random variable z_t. By definition, z_t is i.i.d. on a standardized pdf $\mathscr{F}(0,1)$. Hansen [1994] developed the skewed Student's t distribution for application to leptokurtotic series. Bauwens et al. [2012] suggests asymmetry in the GARCH residuals is necessary to ensure asymmetry in the unconditional distribution. The hypothesis that an eGARCH model with a skewed conditional distribution is capable of describing the assymetry, sign-dependence, and non-linearities of wind power processes is tested in the following sections.

Model Selection and Diagnosis

The regression models in this study are fitted and parameterized using the method of maximum-likelihood estimation (MLE), implemented in the R Statistical Computing package `rugarch` [Ghalanos, 2013]. (R Statistical Computing Language base software and packages are available from http://cran.r-project.org [R Core Team, 2013].) The parameters of the model, described in Table 1, are the estimators that maximize the likelihood function [Akaike, 1998]. Numerous statistical measures based on MLE have been developed to evaluate the suitability of the parameterized

model. This section summarizes the tests used to characterize the GARCH models fitted to hourly net load data.

Parameter selection and significance With any parametric model there is a danger of over-fitting the model by specifying too many parameters and creating a deceptively good fit that fails to reproduce the characteristics of the data in simulations and forecasts [Farrell et al., 1996]. Three tests for testing the parameterization of the model are used below.

1. Standard error and statistical significance: Ghalanos [2013] calculates the t statistics and standard errors (SE) for each of the estimated parameters, along with their robust standard errors, a measure of standard error robust to misspecificaiton of the model, developed by White [1982]. Misspecification of the modeled stochastic process or its probabilistic distribution is often difficult to avoid or to detect a priori. Hipel and McLeod [2004] suggest that if the SE is larger than approximately 1/3 of the estimated parameter the parameter may be considered redundant because the large standard error indicates that the likelihood function is not sensitive to the parameter in question. In the following analysis each estimated parameter is examined for statistical significance and redundancy - SE greater than 10% of the estimated parameter is chosen as a conservative first filter for over-fitting in this case.

2. Nyblom Stability Test: The Nyblom stability test was developed to test the null hypothesis that the parameters of a time series model are constant over time [Nyblom, 1989]. The parameter stability test is implement in Ghalanos [2013] as extended by Hansen [1992] to test the stability of the individual parameters. The test statistics are chi-squared distributed and the null hypothesis that the parameter is stable over various time periods is rejected when the test statistic is greater than the critical value.

3. Akaike Information Criterion (AIC): The AIC is a measure of the relative quality of the fitted model based on the goodness of fit as determined by the log likelihood function and a penalty term based on the number of model parameters [Akaike, 1974]. Among models fitted to the same data set, the model with the lowest AIC is favored over the others.

Overall model fitness Characteristics of the model and its performance in forecasts and simulations should be realistic and consistent with the original properties of the data. Each of these three tests gives insight into whether the model realistically captures specific properties of the data.

1. Persistence and stationarity: Persistence is the notion that a shock or disturbance in the time series will continue to have influence over time that dies out approximately exponentially. In the context that volatility models were developed, persistence with value close to one represents financial risk assumed in the future due to shocks in the past [Nelson, 1991]. More generally, large persistence implies non-stationarity in the variance equation. For each model, the calculated persistence is evaluated with the characteristics of the observed variance in the original data in mind.

2. Unique model parameters: In the comparison of sGARCH to eGARCH, the reason that eGARCH may be preferred is because of asymmetry in the volatility of the data. A statistically significant γ and α parameter estimate verifies the existence of asymmetry in the data and justifies the use of the more sophisticated model.

3. Forecast test: 2400 data points are held back for out-of-sample forecast testing. The mean absolute error (MAE) and mean squared error (MSE) are used to compare the performance of the various models.

Diagnostics The following tests are used determine whether the model is a proper GARCH specification, specifically referring to a valid choice of GARCH model and conditional distribution.

1. Correlation of the squared residuals: Since the stochastic model innovations are generated by $z_t \ (0,1) \, i.i.d$, the squared residuals will have no autocorrelation if the GARCH model is correctly specified. The prevailing test for this correlation is the Ljung-Box Q test [Ljung and Box, 1978], which tests the null hypothesis that the residuals are independently distributed. The Ghalanos [2013] provides Q-statistics for three standard lag values, which are chi-squared distributed, as well as the autocorrelation function for the squared residuals.

2. Remaining ARCH effects: ARCH effects are, stylistically, the autocorrelation of squared residuals. Recalling from equation 3 the ε^2 term is referred to as the ARCH term, refer-

Data set	mean	intercept	slope	Data set	mean	intercept	slope
ln(summer)	8.5037	8.65	-11.0E-6	ln(winter)	8.849	8.8	-8.1E-6
diff(summer)	-0.0141	0.078	-7.0E-6	diff(winter)	-0.0242	0.11	-9.4E-6
summer	5062	5695.4	-0.0478	winter	5871	6400	-0.038

Table 2: Log transformation of the seasonal data set reduced the trend in the raw data comparably to differencing.

ring to the model originally developed in Engle [1982]. The ARCH Lagrange Multiplier (LM) test calculates the test statistic on the squared residuals, which is chi-squared distributed. A well-specified GARCH model will remove all ARCH effects from the residuals.

3. Sign Bias Test: If asymmetry in the volatility of the orginial data was present, there should be no asymmetry remaining in the residuals of the fitted model. The Sign Bias Test of Engle and Ng [1993] is used to determine the whether significant asymmetry remains based on positive shocks, negative shocks, and, jointly, both positive and negative shocks.

Emperical Considerations in GARCH Specification

The following are observable features of the net load timeseries that inform model specifications.

Volatility

The patterns of volatility in net load - that is, clusters of larger changes in series value followed by clusters of smaller changes - and the statistical distribution of data points are markedly different between summer and winter (Figure 4). Wind output is more irregular with lower peaks in the winter months. Summer wind power output is more regular with consistently higher peaks than in winter (Figure 5). Power demand is conversly higher in winter than in summer. Thus, the ratio of peak wind output to peak load increases over the long term, but is higher in winter than in the summer of the same year (this topic is addressed in the next section). In order to account for these differences and more adequately describe the volatility using a GARCH process, the data is divided into two seasonal time series. The seasons are defined to coincide with the power seasons: winter runs from November 1 through April 30, and summer runs from May 1 through October 31.

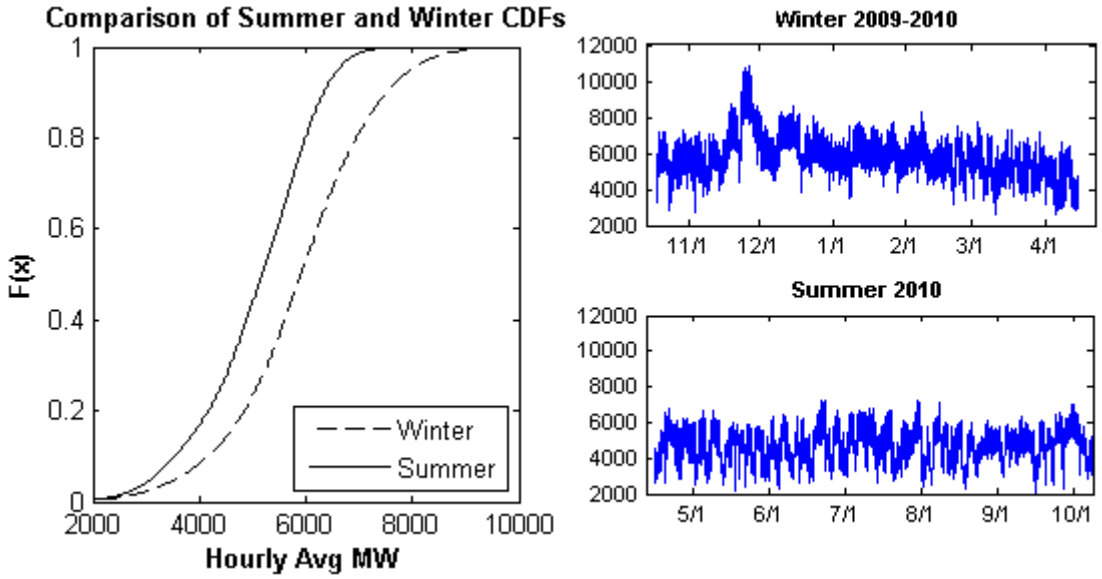

Figure 4: Emperical CDF of net load data by seasons. Winter net load values distributed more widely over the range of net load values due to a high winter peak in the month of January.

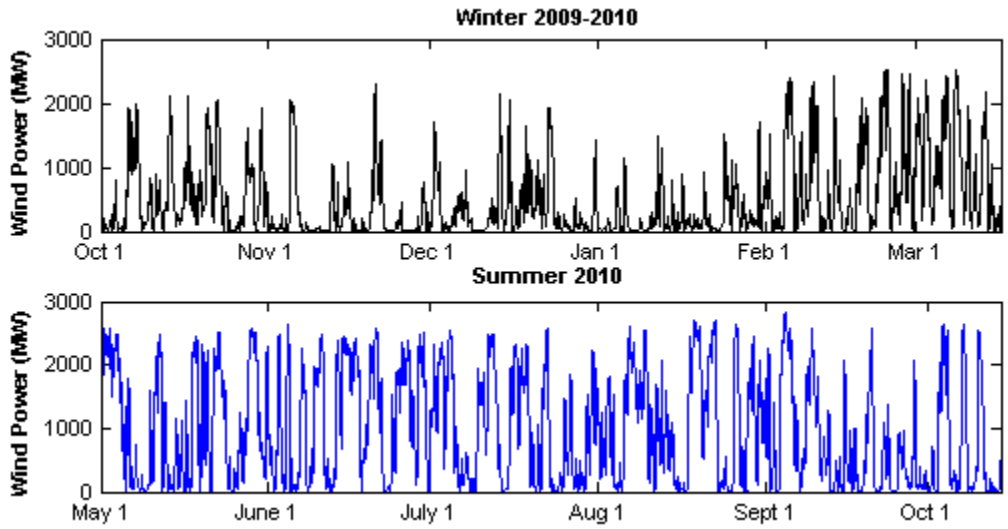

Figure 5: Wind patterns are more regular and more frequently reach full capacity in summer than in winter.

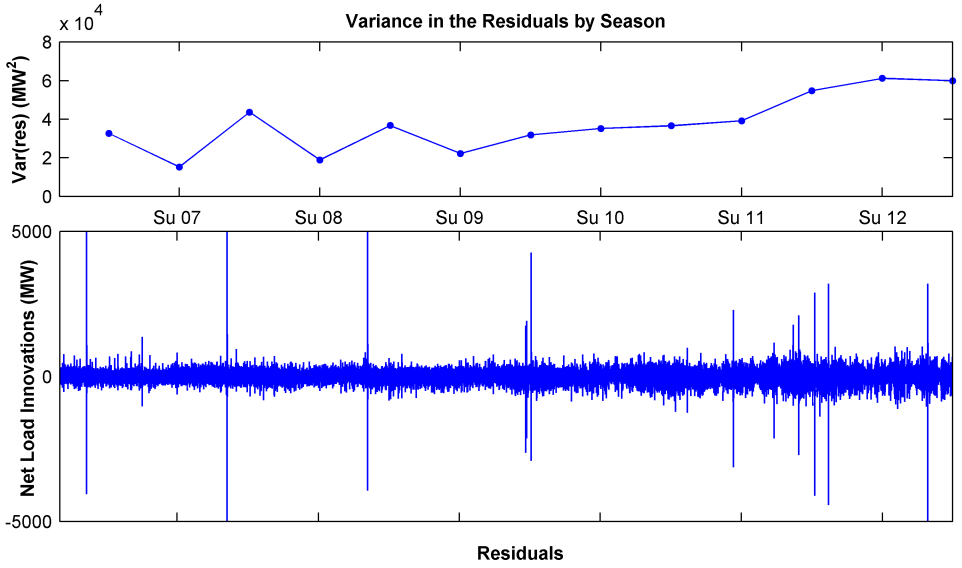

Figure 6: The variance in the residuals, calculated here by season, trends upwards throughout the original sample. The external regressor, wind penetration, explains some of this variance.

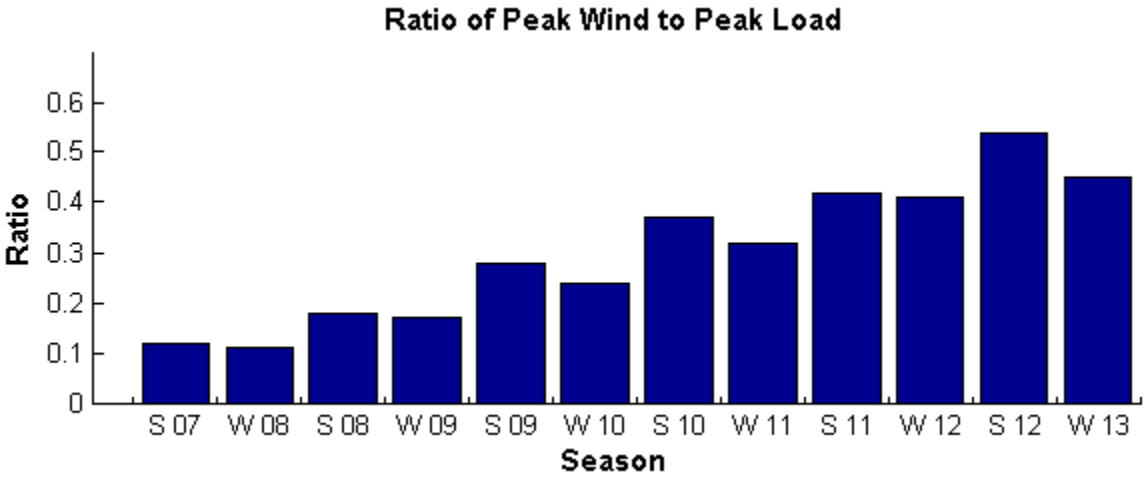

Figure 7: Wind penetration increases over the study period, and is lower in winter than summer due to higher peak load and lower wind outputs.

Trend and Periodicity

ARMA-GARCH models are intended to be fit to data with stationary unconditional mean and variance. This data set has a negative trend in mean net load and a steady increase in the variance (Figure 6). The trend in the mean is shown in Table 2. The increasing variance can be explained by the increases in installed wind generation capacity over the study period. Wind penetration is the quantity used to describe how much wind power is in service relative to the load it serves and can be calculated in terms of annual energy production or in terms of power capacity. In this study, wind power penetration is used, and seasonal peak wind power output is assumed to equal the available installed wind power capacity. Wind penetration is thus defined as $\max(hourly\,wind)/\max(hourly\,load)$ and plotted in Figure 7. In order to explain some of the variance in the data, the model is fitted with wind penetration as an external regressor in the variance equation, described below.

The trend in the mean can be removed by differencing the data once. As an alternative to differencing, a natural log transformation was also tested. The trend in the transformed data is small in magnitude, on the order of 10^{-5} and results in a change over the study period of approximately 2.5 percent of the mean. This approach is considered viable for a GARCH model because there is an annual periodicity in the data that results in local trends in the data that are significantly larger in magnitude than 10^{-5}, causing the overall trend to have a limited effect on the fit of the model. It is shown in Table 2 below that the log-transformed data and differenced data have similar long-term linear trends.

Autocorrelation

The net load time series exhibits strong autocorrelation in both seasons. Figure 8 shows the autocorrelation function (ACF) and partial autocorrelation function (PACF) for the series. The autocorrelation is strong and persistent out past 48 timesteps, and the partial autocorrelation drops off quickly, becoming barely significant after 24 lags. According to Hipel and McLeod [1994], the combination of these two characteristics indicates the need for a mean process model that includes both autoregressive terms (AR) and moving average (MA) terms. The strong ACF and PACF at lags at 8, 18, and 24 hours are indicative of the typical electricity consumption patterns that result

GARCH Process	sGARCH(1,1)	eGARCH(1,1)	eGARCH(1,1)
Mean Process	ARMA(1,1)	ARMA(1,1)	ARMA(2,1)
Conditional Distribution	sstd	sstd	sstd
Regressors	None	None	max wind/max load
Data Set	hourly loads, first difference	hourly loads, first difference	hourly loads, first difference

Table 3: sGARCH and eGARCH were compared in the initial steps of model selection.

in daily peaks at the breakfast and dinner hours correlated with a consumption minimums near 2 am. These observations suggest AR terms between 1 and 24 may be significant, and thus examination of the significance of individual terms is warranted.

Fitted Model

GARCH models were fitted to the net load time series using R package `rugarch` as follows [Ghalanos, 2013].

The sGARCH order (1,1) has been shown to be the best choice for a wide variety of data sets [Bauwens et al., 2012] so sGARCH(1,1) was compared with eGARCH(1,1), fitted to first differenced data. (see Table 3 for model specifications). Five models designed to establish the basic structure of the GARCH formulation were tested. Preliminary analysis had established that a skewed conditional distribution was necessary, and the significance of gamma and the standard errors of alpha and beta clearly indicated that eGARCH was the superior model compared to sGARCH.

The five early model tests included formulations of the mean model utilizing AR(2) and ARMA(2,1) as well as eGARCH(2,1) with and without regressors in the variance model. The complete results are included in Appendix B - Table 1. ARMA(2,1)eGARCH(1,1) with variance regressors outperformed all the other models in all goodness-of-fit measures, including AIC, but failed to remove all sign bias and the Nyblom parameter stability test produced results consistently above the critical value. (See Table 4.) Further refinements were clearly required. At the same time, there are also indications that some ARCH effects remain in the data-squared residuals. ARCH effects are likely, according to the Q test, in the standard residuals. However, in samples this large, that is likely to be the case and squared residuals are considered the more reliable test [Ghalanos, 2013].

The next phase of model selection involved testing data transformations. (See Table 5.) The fit

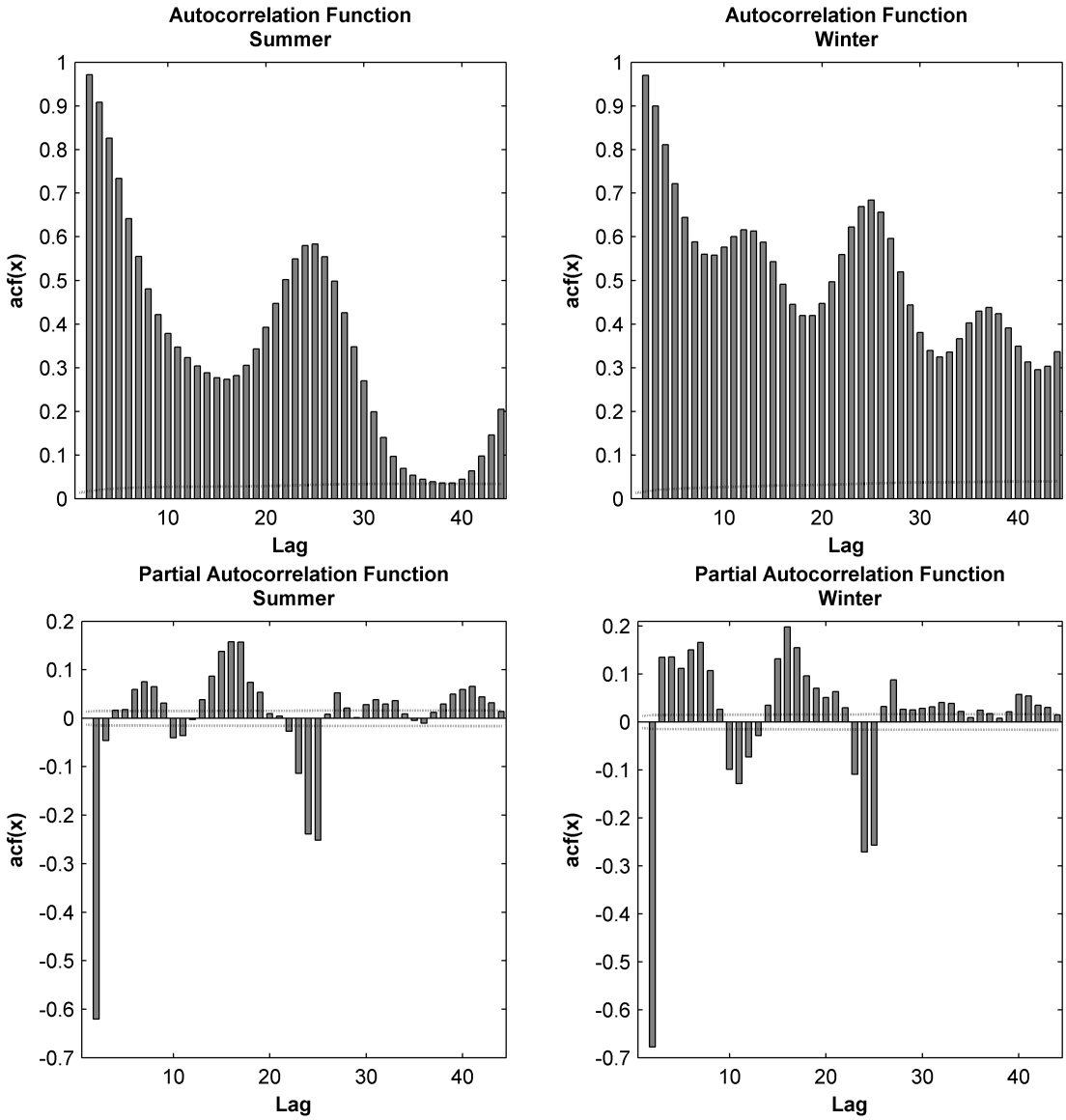

Figure 8: The autocorrelation function and partical autocorrelation function of the seasonal data indicate the need for both AR terms and MA terms.

GARCH Process	sGARCH(1,1)	eGARCH(1,1)	eGARCH(1,1)
Mean Process	ARMA(1,1)	ARMA(1,1)	ARMA(2,1)
AIC	13.39	13.36	13.23
Sign Bias	High Significance	High Significance	Low Significance
Parameter stability	Highly unstable	Highly unstable	γ and skew - <0.47
	β - 63.6		β - 1.7
	shape - 26.0		shape - 3.9

Table 4: Results of the initial models. eGARCH(1,1) with variance regressors was selected to continue with based on AIC, sign bias, and relative improvement in Nyblom parameter stability.

Model ID	10s	11s	15s	15slnreg
GARCH Process	eGARCH(2,1)	eGARCH(2,1)	eGARCH(2,1)	eGARCH(2,1)
Mean Process	ARMA(24,1)	ARMA(24,1)	ARMA(24,1)	ARMA(24,1)
Conditional Dist.	sstd	sstd	sstd	sstd
Regressors	max wind/max load			max wind/max load
Data Set	ln(diff(summer))	ln(diff(summer))	summer	ln(summer)

Table 5: The need for differencing is clear in these comparisons, as well as providing evidence that the natural log transformation improves the ability of the model to capture the more extreme variations in hourly data. The data set summer refers to the hourly data for the summer season described above.

diagnostics for the six models tested are tabulated in Appendix B - Table 2. It was determined that the natural log transformation improved the model fit by improving parameter stability and reducing the magnitude of assymetries so that sign bias was reduced. However, log transformation was not sufficient on its own. In the untransformed data set *summer* and in the log-transformed data, autocorrelations and ARCH effects in the residuals were still very apparent, immediately ruling them out as suitable options and pointing toward the need for differencing. The log-transformed differenced data was selected for detailed model fitting.

Considering the strong daily periodicity of the data, ARMA(24,1)eGARCH(2,1) sstd with regressors fitted to the natural log of the first differenced data was selected as the base model to be refined. The initial model, labeled 10s, performed well, with an AIC of -3.32, no significant sign bias, and highly significant Q statistics indicating uncorrelated residuals. However, nine of the model parameters had standard errors greater than or equal to 0.10 of the estimated value, indicating the model is "over fit." So model 10s was altered systematically, removing or adding one parameter at a time using the partial autocorrelation function as guidance. "Removing" a parameter out of sequence is accomplished in rugarch by setting the parameter to have a fixed value of zero. 14 modifications of Model 10s were tested and a subset of the summer models are summarized in the results section below. Building on the patterns observed in the summer trials, winter parameterization was more targeted, with a total of seven combinations of parameters tested. A summary of this procedure is provided in Appendix B - Table 3.

Model ID	Model	AIC
10s	ARMA(24,1)	-3.32
10s4	ar={1,2,6,24}	-3.25
10s8	ar={1,2,6,14,15,16,23,24}	-3.3
1w	ARMA(24,1)	-3.63
5w	ar={1,2,6,16,17}	-3.3
7w	ar={1,2,6,24}	-3.51

Table 6: For each data set, summer and winter, one or more reduced models performed as well as the model based on eGARCH(2,1)ARMA(24,1), but achieved a lower AIC and improved parameter significance.

Selected Models

In the case of both winter and summer, the ARMA(24,1)eGARCH(2,1) models performed well in all general measures of goodness of fit. Compared with all models tested, the AIC was low, sign bias was eliminated, and serial correlations and ARCH effects were removed. However, a number of parameters were statistically insignificant or had high standard errors, indicating the risk of over-fitting. Through the process described above, the model parameter estimates were improved and the best three seasonal models are listed in Table 6. These models were selected because of their significant parameters and low AICs, as well as passing the rest of the goodness of fit tests, to be compared in forecast tests, applied in the next section.

The Nyblom stability parameters were often above the critical value for several parameters in each of the models. This is not unexpected because the data series being fitted are somewhat longer than they should be. It is important to note, however, that the distribution parameters, skew and shape, are within the critical value, or nearly so, for each of the models selected for forecast tests, indicating a stable conditional distribution for the GARCH model across the entire sample. For the forecast test, models with the most stable conditional distribution parameters were preferred.

The persistence for an eGARCH model is defined to be the sum of the beta parameters [Ghalanos, 2013]. In each of the selected models, β is less than one. As expected, the inclusion of variance regressors that explain the steady increase in variance due to increased wind penetration reduces the value of β somewhat.

Forecast Experiments

Each model regression using the `rugarch` package creates a fit object that includes a specification of data held out for the purposes of out-of-sample forecast tests. The size of the out sample was selected based on the seasonality of the series being fit: the last one-half season of summer and the last full season of winter were held out. The difference is in the desire to see whether there was a drastic difference in forecast error when data representative of the season being forecast was present in the data fit.

The forecast method in `rugarch` takes a fit object which specifies an out sample of length n. The forecast is a rolling forecast, with single period look ahead, and $n-1$ rolls. In this forecast experiment, wind penetration from the last year in the time series, the year with the largest wind penetration, was utilized as the regression data.

The forecast object is returned with forecast error measures - mean squared error (MSE), mean absolute error (MAE), and the Directional Accuracy Test (DAT), which provides a measure of how often the value of the model changed in the same direction as the original data set. In a comparison, the model with the lowest MSE and MAE and highest DAT is the superior model for forecasting.

Table 7 summarizes the forecast results. Each of the best models described above were tested, with the exception of model 5w, which exhibited unstable conditional distribution parameters in spite of its superior AIC value. The models performed similarly, with the "overfit" 10s and 1w models scoring very slightly better. In comparison with each other, the low variance in the MSE and MAE suggests that the other model diagnostics should be the deciding factor. Note the difference between MSE in the summer models and winter models: Including a portion of the forecasted season made a sizeable difference in the MSE, suggesting the regression in the variance equation was not fully effective in capturing the inter-annual dynamics.

Simulation of Data

The following simulated data set was generated from the models selected in the forecast test - specifically Model 10s8 and Model 7w. The simulated mean series values were transformed back

Model ID	MSE	MAE	DAT
10s8	0.004149	0.04617	1
10s4	0.004294	0.04705	1
10s	0.004078	0.04560	1
1w	0.006150	0.04370	1
7w	0.006860	0.04637	1

Table 7: A rolling forecast over the last season of historical data was performed on each of the models selected in the previous section. The detailed forecast specifications can be found in Appendix B - Table 4.

to differenced MW values, with $x_0 = 0$. Simple integration of the differenced series resulted in a series with a large amount of departure from x_o due to the compounding of estimation error over the integration. The mean squared error of any single simulated observation can be calculated using the random-shock moving average equivalent of the ARIMA model [Hipel and McLeod, 1994], using

$$MSE = \sigma_l^2 + \psi_1^2\sigma_{l-1}^2 + ... + \psi_{l-2}^2\sigma_2^2 + \psi_{l-1}^2\sigma_1^2$$

where l is the number of timesteps beyond $t = 0$, σ_t^2 is the conditional variance at time t, and ψ_i is the ith Psi-weight of the random-shock model representation [Hipel and McLeod, 1994]. In a homoskedastic process, $\sigma_t^2 = \sigma_{t+1}^2$ for all t, and the MSE approaches the unconditional variance of the series for long time horizons. The prediction errors for predicted values beyond $t = 0$, given uncorrelated errors, can be shown to be correlated [Box and Jenkins, 1976]. However, in this GARCH model the errors are time dependent and serially correlated, and the Psi-weights diminish slowly over time, characterized by a 24-hour periodicity and retaining relatively large positive values at the 24-hour interval beyond 100 time stepes resulting in the trend in the simulated data.

To remove the cumulative effect of the correlation in error terms, the following algorithm was developed to filter the long-term effects from the integrated series. In particular, filter sizes were selected to cover the strongest peaks in the Psi-weights within two 24-hour periods of the simulated value. For the summer series, the strong peaks are located at t+24 hours, while for the winter series, the peaks at t+12 and t+24 were similar in value. The filter used was a simple moving average, centered on the simulated value. The moving average value was subtracted from the integrated simulated values, resulting in a demeaned simulated series.

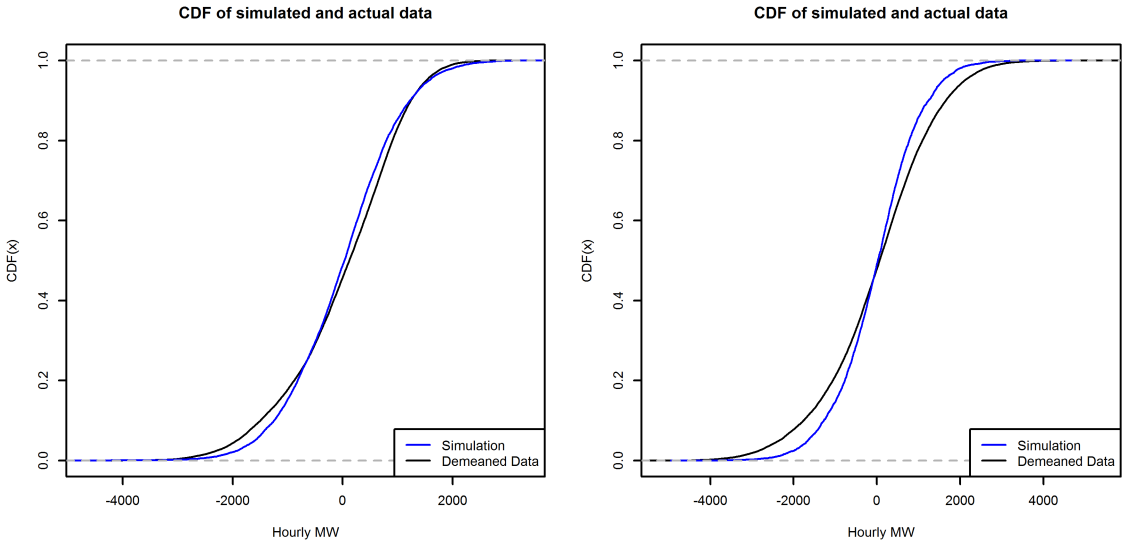

Figure 9: The CDF of simulated values confirm that the low-pass filter used to de-mean the data preserved the statistics of the original simulation for the summer data set (left) and the winter data set (right).

The distributions of the simulated series and the original, demeaned data are compared to evaluate the success of this approach. In Figure 9 the CDF of the summer simulation confirms the results of the original fit: the simulated values are well-distributed over most of the distribution, with the exception of the lower tail, which is "light." The winter simulation is precisely the right shape but is light in both tails. However, the innovations of the summer and winter simulations are skewed toward the tails compared to the original data (Figure 10), an apparently contradictory observation that is explained by comparing a section of the two timeseries. Qualitatively, Figure 11 compares the summer simulation and original net load data from summer, 2012. The original data displays pronounced low-variance periods of high values corresponding to calm, low-wind conidtions, and high-variance periods with relatively low values, corresponding to windy conditions. The simulated mean data do not retain this anti-correlation between variance and value. However, plotting prediction intervals depicting the distribution of values for each time step, as described by the simulated conditional standard deviation, the anti-correlation becomes visually apparent in the assymetric distribution of simulated values (Figure 12).

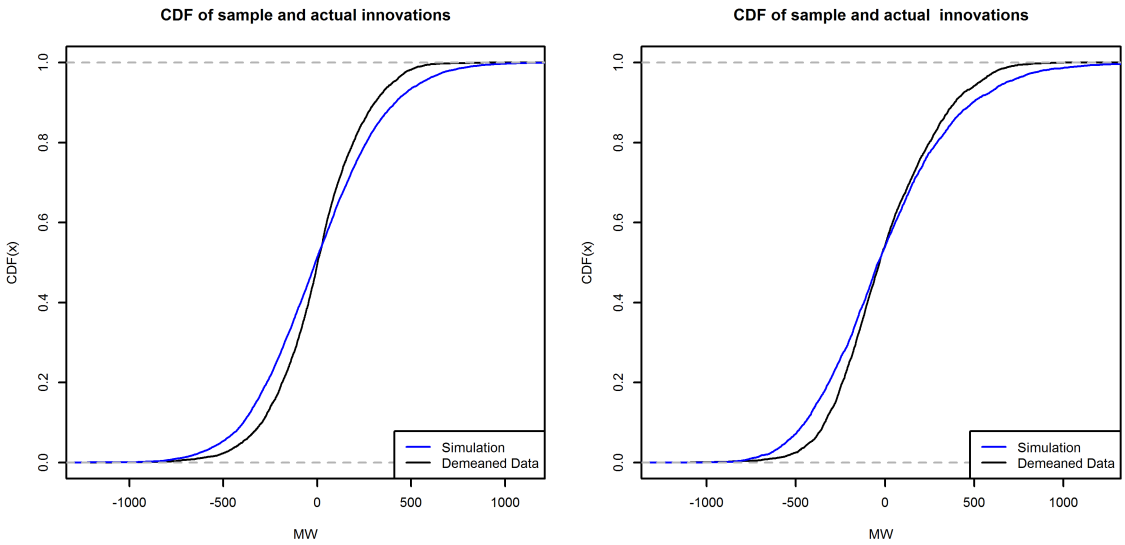

Figure 10: The innovations in the summer (left) and winter (right) simulations are skewed toward the tails of the distribution.

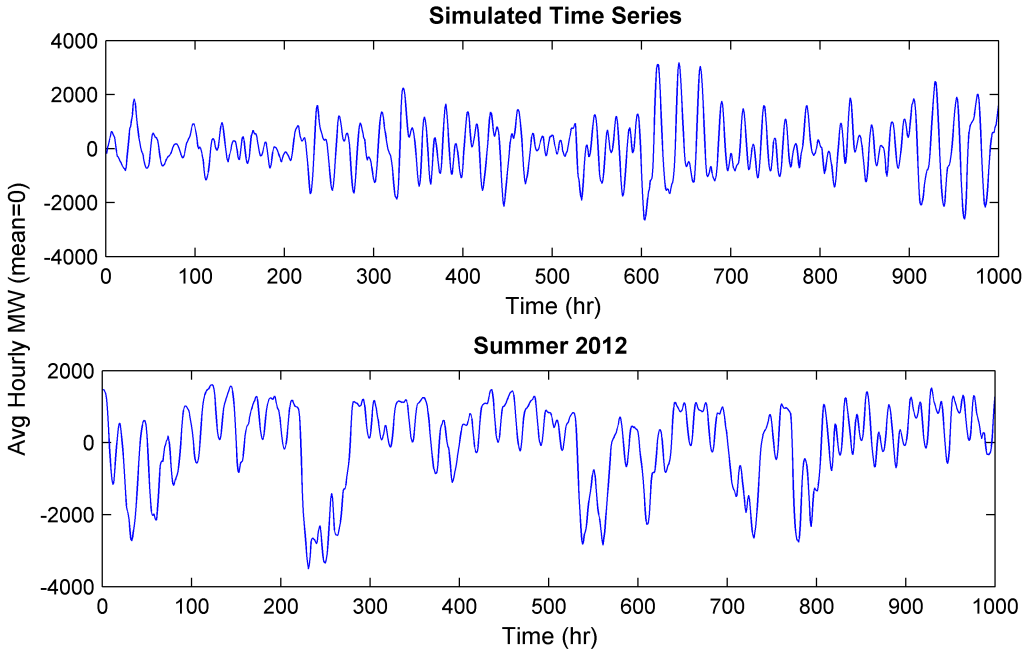

Figure 11: A comparison of a portion of the simulated series and the original data shows that the simulation successfully captures high and low volatility periods, but the anti-correlation between series value and local volatility is not apparent. This feature becomes apparent when confidence intervals are added to the plot (see Figure 12).

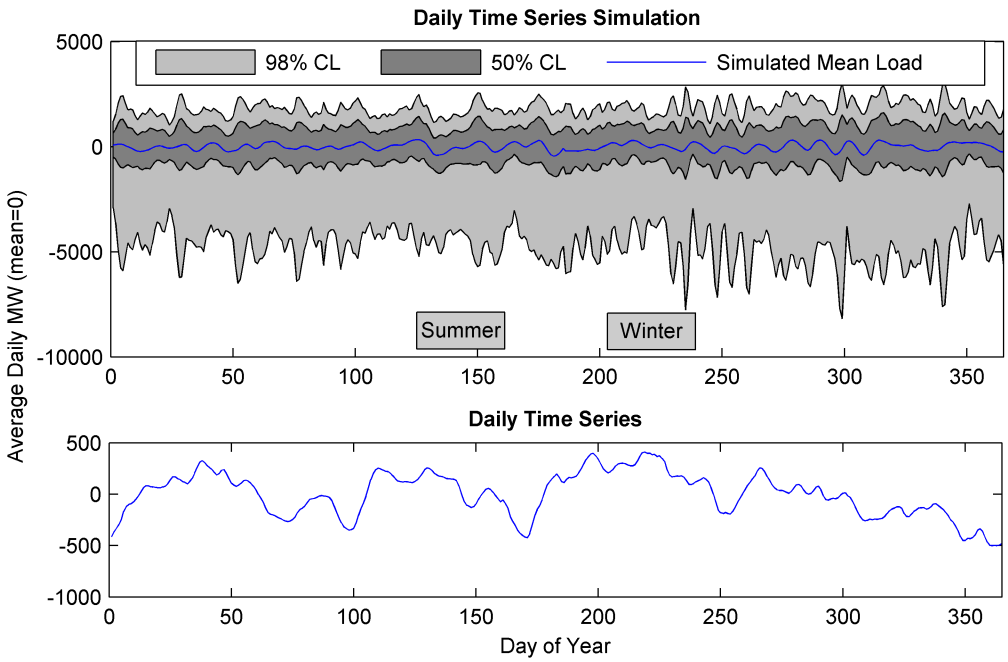

Figure 12:

Conclusions

Electricity demand, or load, is a stochastic input that is important in a number of fianancial and operational models. Increasingly, wind power is a second stochastic quantity that must be taken into account, and which is likely to include a trend in both its magnitude and variability. Combining the two quantities serves to obscure some of the individual process dynamics, as well as the possible correlations between wind power output and total demand such as weather effects, time of day, and scheduling decisions. In the same way that GARCH modeling was originally developed to cope with similar “micro processes” in financial returns, the objective of this study is to demonstrate that GARCH modeling is a useful tool for modeling the dynamics of regional net load utilizing only readily available data, and to develop synthetic simulations useful for both static and dynamic modeling. Multiple model formulations were found that passed the selected goodness of fit measures, performed similarly in forecasting tests, and produce useful simulations.

It was confirmed in the model fitting and testing that a subset of the ARMA(24,1) mean model is needed to capture the periodicity of the net load series. The AR24 parameter was not stable according to the Nyblom stability test for all models tested, but its inclusion improved the other

fit measures of the model compared to excluding it. The two models selected for the simulation included AR terms at lags 1,2,6 and 24 which resulted in highly significant parameters, passed the goodness of fit tests, and resulted in similar or superior stability measures compared to the similar models.

Using wind penetration as a regression variable in the variance, the simulation successfully reproduced the change in variance from one year to the next. However, the correlation with wind penetration was not strong enough so that the magnitude of the change in variance was captured effectively. Some of this effect is due to a wide range of net load conditions within each of the two seasons of the model. A seasonal model developed on monthly or quarterly data may be more able to capture the relative changes in variance associated with wind penetration.

In the next chapter, the simulated data will be used to calculate the economically optimal pumped-storage hydropower investment given an existing regional supply curve. It will be shown how some of the noise in the hourly GARCH simulation can be mitigated by aggregating the hourly simulated data into longer timesteps. In Chapter 4, the same simulated data at the hourly resolution and the results of Chapter 3 are used to dynamically simulate the operations of pumped storage under uncertainty and determine the sensitivity of operations to changes in net load variance.

Appendix A

A number of variations of the standard GARCH model have been developed to capture the non-linear and assymetric properties of series variance.

N-GARCH - The non-linear GARCH model was developed by Engle and Ng [1993] to capture the leverage effect of current innovations on future volatility by introducing an extra term in the ARCH expression:

$$\sigma_t^2 = \beta\sigma_{t-1}^2 + \alpha(\varepsilon_{t-1} - \theta\sqrt{\sigma^2})^2$$

whereα is the ARCH term, β is the GARCH term, ε is the series innovation defined as $\varepsilon_t = \sigma_t z_t$ as above, and θ is the leverage term.

Q-GARCH - Quadratic GARCH was first proposed by Sentana [1995] to model the asymmetric effects of both positive and negative innovations.

$$\sigma_t^2 = \beta\sigma_{t-1}^2 + \alpha\varepsilon_{t-1}^2 + \phi\varepsilon_{t-1}.$$

GJR-GARCH, a model developed by Glosten, et al. [1993] implements the indicator function, I_{t-j}, to model positive and negative shocks assymetrically.

$$\sigma_t^2 = \sum_{j=1}^{q}(\alpha_j\varepsilon_{t-j}^2 + \gamma_j I_{t-j}\varepsilon_{t-j}^2) + \sum_{j=1}^{p}\beta_j\sigma_{t-j}^2$$

where the indicator function I takes the value 1 for $\varepsilon > 0$ and 0 otherwise, and γ is referred to as the leverage term because it corresponds to the disproportional influence that a positive innovation will have on future variance compared to negative innovations.

Appendix B

All parameter estimates and significance tests were evaluated based on the outputs contained in the tables below. These outputs were produced by the `ugarchfit` method from the `rugarch` package for R [Ghalanos, 2013; R Core Team, 2013]. Each fit object was given an ID indicating the season (s, w), the model run number, and whether the variance model included external regressors (reg).

Diss

GARCH	sGARCH(1,1)				eGARCH(1,1)				eGARCH(1,1)				eGARCH(1,1)				eGARCH(1,1)			
Mean	ARMA(1,1)				ARMA(1,1)				AR(2)				ARMA(2,1)				ARMA(2,1)			
Dist	sstd				sstd				sstd				sstd				sstd			
Regressors																	xternal reg: max wind/max load			
Data Set	diffhourlyload				diffhourlyload				diffhourlyload				diffhourlyload				diffhourlyload			
Parameters																				
	Estimate	**Std Error**	**t value**	**Pr(>|t|)**	**Estimate**	**Std Error**	**t value**	**Pr(>|t|)**	**Estimate**	**Std Error**	**t value**	**Pr(>|t|)**	**Estimate**	**Std Error**	**t value**	**Pr(>|t|)**	**Estimate**	**Std Error**	**t value**	**Pr(>|t|)**
mu	-1.99166	2.089794	-0.95304	0.34057	1.99149	0.693698	2.8708	0.004094	1.99064	2.949768	0.67485	0.49977	1.99164	0.727319	2.7383	0.006175	1.92502	0.682973	2.8186	0.004824
ar1	0.58346	0.004538	128.568	0	0.5883	0.004233	138.9918	0	0.93305	0.004795	194.581	0	1.6277	0.003504	464.4786	0	1.63062	0.003399	479.7256	0
ar2									-0.28912	0.004169	-69.3477	0	-0.74459	0.002695	-276.24	0	-0.74675	0.002734	-273.154	0
ma1	0.30779	0.004999	61.57193	0	0.286	0.00555	51.5308	0					-0.89334	0.004839	-184.606	0	-0.90029	0.003713	-242.471	0
omega	15849.81	411.7133	38.49721	0	3.54857	0.08132	43.6373	0	3.96197	0.090537	43.7609	0	4.04153	0.096534	41.8663	0	4.19719	0.099373	42.2368	0
alpha1	0.44474	0.012644	35.173	0	0.23325	0.006544	35.6446	0	0.22599	0.007424	30.44241	0	0.19225	0.007354	26.142	0	0.1988	0.007443	26.7117	0
beta1	0.2922	0.010481	27.87869	0	0.66512	0.007651	86.9339	0	0.62584	0.008551	73.18442	0	0.61664	0.009144	67.4371	0	0.57587	0.009962	57.8056	0
gamma1					0.58491	0.011747	49.7919	0	0.63653	0.01226	51.91962	0	0.63642	0.012354	51.5158	0	0.61447	0.012509	49.1207	0
vxreg1																	0.89918	0.041516	21.6586	0
skew	1.00188	0.005708	175.5339	0	1.00914	0.005499	183.5041	0	1.0181	0.006441	158.0636	0	0.96085	0.005623	170.8908	0	0.95554	0.005759	165.93	0
shape	5.24627	0.125353	41.85186	0	5.38915	0.126884	42.4729	0	5.01744	0.113397	44.24671	0	4.70837	0.104557	45.0315	0	4.85406	0.111606	43.4927	0
Log Likelihood	-367869				-367047				-366333				-364381				-353898			
AIC	13.39				13.36				13.334				13.263				13.233			
Q-stats on Standard Residuals																				
	Q Stat	**p-value**			**Q Stat**	**p-value**			**Q Stat**	**p-value**			**Q Stat**	**p-value**			**Q Stat**	**p-value**		
Lag[1]	8.999	0.002701			11.51	0.000692			72.45	0		Lag[1]	103.1	0			151.7	0		
Lag[p+q+1][3]	400.929	0			382.56	0			173.49	0		Lag[4]	264.8	0			330.9	0		
Lag[p+q+5][7]	3746.121	0			3878.43	0			2384.52	0		Lag[8]	1161.2	0			1326.9	0		
d.o.f=2																				
Ho: No serial correlation																				
Q-stats on Squared Residuals																				
Lag[1]	2.321	0.1276			0.121	0.728			0.3206	0.5713			0.7857	0.3754			0.2949	0.5871		
Lag[p+q+1][3]	2.627	0.1051			0.2785	0.5977			0.4337	0.5102			1.0305	0.31			0.3977	0.5283		
Lag[p+q+5][7]	3.962	0.5548			1.0134	0.9615			1.0578	0.9578			1.7764	0.8791			0.9265	0.9683		
d.o.f=2																				
ARCH LM Test		**p-value**				**p-value**				**p-value**				**p-value**						
ARCH lag[2]	2.591	0.2737			0.279	0.8698			0.4344	0.8048			1.012	0.603			0.384	0.8253		
ARCH lag[5]	3.764	0.5839			0.9299	0.968			0.9643	0.9654			1.714	0.8871			0.918	0.9689		
ARCHlag[10]	4.162	0.9397			1.2444	0.9995			1.3051	0.9994			2.39	0.9924			1.182	0.9996		
Nyblom stability test		**5% Critical Value**				**5% Critical Value**				**5% Critical Value**				**5% Critical Value**				**5% Critical Value**		
Joint Stat	105.9658	> 2.11			109.275	> 2.32			127.8706	> 2.32			145.4388	> 2.54			63.9547	> 2.75		
mu	3.311	> 0.47			5.283	> 0.47			2.543	> 0.47			10.3285	> 0.47			4.1608	> 0.47		
ar1	11.566				8.784				4.854				12.6145				13.2606			
ar2													19.6331				19.8723			
ma1	22.791				19.561				2.377				9.5456				9.8138			
omega	45.81				58.954				65.105				71.9455				2.0426			
alpha1	31.371				24.355				22.779				20.022				14.9599			
beta1	63.627				60.535				67.417				74.5769				2.2895			
gamma1					1.119				1.28				2.8204				0.2924			
vxreg1																	1.6791			
skew	1.278				2.376				1.255				0.2652				0.2821			
shape	26.003				13.63				21.414				31.7996				3.851			
Sign Bias Test																				
Sign Bias	**																			
Negative Sign Bias	**																			
Positive Sign Bias					***				***				**				**			
Joint Effect	***				***				**				***				*			

Sign Bias, testing the null hypothesis that no asymmetry remains in the residuals - * = reject the null with low significance, ** = moderate significance, *** = high significance

Table 2 - Results from data transformation study and corresponding fit diagnostics

GARCH	eGARCH(2,1)			10s	eGARCH(2,1)			11s	eGARCH(2,1)			15s	eGARCH(2,1)			15slnreg
Mean	ARMA(24,1)				ARMA(24,1)				ARMA(24,1)				ARMA(24,1)			
Dist	sstd				sstd				sstd				sstd			
Regressors	xternal reg: max wind/max load												xternal reg: max wind/max load			
Data Set	Indiffsummer				Indiffsummer				summer				lnsummer			
Parameters																
	Estimate	**Std Error**	**t value**	**Pr(>|t|)**	**Estimate**	**Std Error**	**t value**	**Pr(>|t|)**	**Estimate**	**Std Error**	**t value**	**Pr(>|t|)**	**Estimate**	**Std Error**	**t value**	**Pr(>|t|)**
mu	8.062822	0.000265	30470.71	0	8.062753	0.000385	20968.13	0	5399.459	40.74938	132.5	0	8.594201	0.007255	1184.579	0
ar1	0.342799	0.013955	24.56469	0	0.343829	0.013718	25.06364	0	1.957479	0.001375	1424.1	0	1.952059	0.001645	1186.833	0
ar2	0.011922	0.008302	1.43591	0.151027	0.012133	0.009051	1.34046	0.180095	-1.29658	0.002223	-583.25	0	-1.2973	0.002199	-590.037	0
ar3	-0.03564	0.005248	-6.7921	0	-0.03381	0.004369	-7.73948	0	0.35173	0.003418	102.91	0	0.347837	0.003012	115.4903	0
ar4	-0.00817	0.004466	-1.82956	0.067315	-0.00847	0.004402	-1.92416	0.054335	-0.00601	0.001968	-3.0527	0.002268	0.00131	0.002073	0.63199	0.527395
ar5	-0.02985	0.005197	-5.74316	0	-0.02966	0.004342	-6.82998	0	-0.03649	0.002137	-17.073	0	-0.03951	0.001651	-23.9248	0
ar6	-0.05454	0.005562	-9.80546	0	-0.05393	0.004489	-12.0131	0	-0.01506	0.002138	-7.0406	0	-0.01273	0.001178	-10.8069	0
ar7	-0.04882	0.005561	-8.77969	0	-0.04863	0.004316	-11.2665	0	0.02962	0.003833	7.7284	0	0.030706	0.004121	7.45129	0
ar8	-0.0792	0.005266	-15.0401	0	-0.07893	0.004764	-16.5673	0	-0.05638	0.002437	-23.131	0	-0.0471	0.004802	-9.80869	0
ar9	-0.01235	0.005512	-2.24088	0.025034	-0.01327	0.004249	-3.12306	0.00179	0.099532	0.000836	119.13	0	0.09234	0.002183	42.29476	0
ar10	-0.00384	0.005286	-0.72656	0.467493	-0.00431	0.004729	-0.91048	0.36257	-0.03932	0.002406	-16.343	0	-0.04807	0.002768	-17.3703	0
ar11	-0.00704	0.004891	-1.43926	0.150078	-0.00582	0.003911	-1.48738	0.136914	0.001544	0.004454	0.34672	0.728804	0.002352	0.001069	2.19978	0.027822
ar12	-0.00435	0.004422	-0.98462	0.324808	-0.00376	0.004787	-0.78458	0.432699	0.003325	0.001476	2.2522	0.024308	0.005245	0.000667	7.86532	0
ar13	-0.0271	0.004231	-6.40444	0	-0.0277	0.005057	-5.47641	0	-0.02579	0.001145	-22.527	0	-0.02205	0.000729	-30.2663	0
ar14	-0.04121	0.005027	-8.19771	0	-0.03973	0.005213	-7.62187	0	-0.00255	0.002091	-1.2185	0.223023	-4.6E-05	0.000178	-0.26135	0.793825
ar15	-0.04559	0.005323	-8.56439	0	-0.04557	0.0047	-9.69715	0	0.002699	0.002094	1.289	0.197387	0.003802	0.001308	2.90739	0.003645
ar16	-0.0577	0.00509	-11.3371	0	-0.05652	0.005426	-10.4161	0	-0.02867	0.002084	-13.756	0	-0.02941	0.001687	-17.434	0
ar17	-0.01901	0.004418	-4.30203	0.000017	-0.01889	0.004961	-3.80766	0.00014	0.073319	0.002073	35.364	0	0.062618	0.001621	38.6406	0
ar18	-0.01803	0.004501	-4.00594	0.000062	-0.01805	0.004898	-3.68588	0.000228	-0.0424	0.003291	-12.884	0	-0.04184	0.001654	-25.2935	0
ar19	-0.00531	0.004608	-1.15233	0.249184	-0.00585	0.00434	-1.34858	0.177473	0.033645	0.004555	7.3869	0	0.038771	0.001641	23.62023	0
ar20	-0.00554	0.004468	-1.24007	0.214948	-0.00398	0.003829	-1.03852	0.299026	-0.01704	0.002151	-7.9215	0	-0.01949	0.001142	-17.0696	0
ar21	-0.0305	0.004385	-6.95586	0	-0.02942	0.004279	-6.87636	0	-0.03225	0.00513	-6.2865	0	-0.02664	0.001269	-20.9916	0
ar22	-0.01609	0.004775	-3.36898	0.000754	-0.01644	0.003241	-5.07131	0	0.01941	0.002233	8.6911	0	0.026696	0.001181	22.611	0
ar23	0.119275	0.005115	23.31664	0	0.119823	0.004643	25.80768	0	0.260864	0.001445	180.53	0	0.235794	0.004709	50.06806	0
ar24	0.306812	0.000971	315.8659	0	0.304303	0.006451	47.17313	0	-0.24778	0.001878	-131.94	0	-0.22957	0.003445	-66.648	0
ma1	0.169042	0.014063	12.02024	0	0.16837	0.013661	12.32464	0	-0.43134	0.006742	-63.983	0	-0.41942	0.006483	-64.6969	0
omega	-0.29072	0.012832	-22.6552	0	-0.0772	0.000536	-144.037	0	0.098458	0.000551	178.68	0	-0.26461	0.006658	-39.7421	0
alpha1	-0.02285	0.011075	-2.06309	0.039104	-0.0283	0.012085	-2.34151	0.019206	0.002228	0.011926	0.18683	0.851794	-0.03798	0.012062	-3.14845	0.001641
alpha2	0.016659	0.010627	1.56768	0.116955	0.028893	0.011811	2.44631	0.014433	-0.02962	0.012064	-2.4555	0.014069	-0.05516	0.011975	-4.60649	0.000004
beta1	0.959083	0.001815	528.4479	0	0.987131	0.000032	31197.78	0	0.990158	0.000004	229260	0	0.967132	0.000924	1047.014	0
gamma1	0.496014	0.016264	30.49833	0	0.499449	0.0169	29.55377	0	0.500917	0.015546	32.222	0	0.532247	0.016188	32.87815	0
gamma2	-0.39025	0.015911	-24.5278	0	-0.40658	0.016694	-24.355	0	-0.41726	0.015787	-26.43	0	-0.39698	0.014911	-26.6232	0
vxreg1	0.146779	0.009623	15.25351	0									0.109925	0.007925	13.86979	0
skew	0.881989	0.00715	123.3503	0	0.880078	0.005113	172.1308	0	0.938328	0.008384	111.92	0	0.943437	0.008888	106.1497	0
shape	4.433836	0.145606	30.451	0	4.298738	0.120425	35.69637	0	4.606561	0.138912	33.162	0	4.755912	0.152038	31.28115	0
Log Likelihood	40076.43				39953.74				-154535				50307.44			
AIC	-3.3236				-3.3135				12.829				-4.1727			

Continued on the next page

Table 2 continued - Results from data transformation study and corresponding fit diagnostics

GARCH	eGARCH(2,1) 10s	eGARCH(2,1) 11s	eGARCH(2,1) 15s	eGARCH(2,1) 15slnreg
Mean	ARMA(24,1)	ARMA(24,1)	ARMA(24,1)	ARMA(24,1)
Dist	sstd	sstd	sstd	sstd
Regressors	xternal reg: max wind/max load			xternal reg: max wind/max load
Data Set	Indiffsummer	Indiffsummer	summer	lnsummer
Q-stats on Standard Residuals				
	Q Stat p-value	**Q Stat p-value**	**Q Stat p-value**	**Q Stat p-value**
Lag[1]	5.399 0.02014	3.292 0.06961	43.84 3.56E-11	47.71 4.94E-12
Lag[p+q+1][26]	270.872 0	263.596 0	1220.58 0	1181.4 0
Lag[p+q+5][30]	328.353 0	323.306 0	1296.75 0	1265.13 0
d.o.f=2				
Ho: No serial correlation				
Q-stats on Squared Residuals				
Lag[1]	8.11E-06 0.9977	1.7E-06 0.999	0.4122 0.5209	0.01412 0.90542
Lag[p+q+1][4]	0.002645 0.959	0.002473 0.9603	475.8235 0	15.03756 0.000105
Lag[p+q+5][8]	0.006076 1	0.00616 1	478.8508 0	16.86502 0.004763
d.o.f=2				
ARCH LM Test	**p-value**	**p-value**	**p-value**	
ARCH lag[2]	0.000192 0.9999	1.21E-05 1	474.3 0	14.52 0.000702
ARCH lag[5]	0.004315 1	0.004257 1	484.4 0	16.03 0.006759
ARCHlag[10]	0.008579 1	0.008864 1	484.7 0	16.93 0.075956
Nyblom stability test	**5% Critical Value**	**5% Critical Value**	**5% Critical Value**	**5% Critical Value**
	> 0.47	> 0.47	> 0.47	> 0.47
mu	0.1902	0.04367	4.2347	5.2584
ar1	0.5375	0.68319	2.1434	0.8381
ar2	0.7264	0.81642	1.4717	0.6494
ar3	2.1129	2.23396	0.8446	0.4092
ar4	1.4801	1.47982	0.3932	0.2406
ar5	0.3216	0.35534	0.2125	0.233
ar6	2.0456	2.07445	0.1443	0.2742
ar7	0.2302	0.2115	0.1539	0.3899
ar8	2.5251	2.40832	0.2117	0.4928
ar9	0.3539	0.29618	0.3665	0.7146
ar10	0.3293	0.28496	0.4785	0.8293
ar11	0.5712	0.52828	0.6482	1.0015
ar12	0.5445	0.56606	0.8388	1.1776
ar13	0.3724	0.36901	1.0516	1.3829
ar14	1.0111	1.01859	1.3098	1.658
ar15	0.8683	0.90365	1.7245	2.1455
ar16	1.4277	1.51906	2.18	2.7848
ar17	0.0542	0.05403	2.5506	3.4695
ar18	0.1264	0.11971	2.5217	3.7442
ar19	0.4741	0.609	2.443	3.9745
ar20	0.3703	0.41232	2.0541	3.6594
ar21	0.1121	0.10878	1.685	3.1396
ar22	1.2572	1.39829	1.1473	2.1552
ar23	4.9091	4.9375	0.3862	0.753
ar24	18.9615	18.92843	0.1004	0.1031
ma1	6.1547	6.39354	14.1393	10.2201
omega	0.2185	10.86375	2.6464	0.2334
alpha1	2.7606	4.57018	6.6414	8.8574
alpha2	2.6344	4.9802	5.8508	7.8974
beta1	0.2622	10.78662	2.767	0.3263
gamma1	3.1486	3.38145	1.6444	6.1965
gamma2	5.1667	4.28779	4.0545	11.8416
vxreg1	0.1808			0.2342
skew	0.5729	0.8968	1.2738	1.2611
shape	0.201	3.03328	1.952	1.0338
Sign Bias Test				
Sign Bias	0.2695	0.2801	0.8287	0.7365
Negative Sign Bias	0.8802	0.9891	5.06E-13 ***	0.0682 *
Positive Sign Bias	0.7257	0.7758	4.12E-08 ***	0.9155
Joint Effect	0.7438	0.7367	3.94E-18 ***	0.1514

Sign Bias, testing the null hypothesis that no asymmetry remains in the residuals - * = reject the null with low significance, ** = moderate significance, *** = high significance

Table 3 - Summary of steps toward model refinement

Progression of Models - Summer			
Model ID	**Fixed parameter models: building on fit10s**	**AIC**	**Notes**
fit10s	eGARCH(2,1) ARMA(24,1) sstd reg	**-3.32**	All perform well in terms of model diagostic measures, but have too many parameters
fit10s1	ar1,2,24,48 and ma1, eGARCH(2,1)	**-3.3**	AIC = -3.3; gamma2 insignificant; ar24 and ar48 not stable. Use eGARCH(1,1) in subsequent models.
fit10s2	ar1,2,24, and ma1	**-3.23**	AIC= -3.23; alpha1 not significant; ar24 not stable
fit10s3	ar1,2,3,24, and ma1	**-3.23**	AIC= -3.23; same as 10s3
fit10s4	ar1,2,6,24, and ma1	**-3.25**	AIC= -3.25; good parameter significance; ar24 unstable;
fit10s5	ar1,2,6,16,24, and ma1	**-3.25**	No improvement
fit10s6	ar1,2,6,16,23,24, and ma1	**-3.297**	AIC= -3.297; slight improvement in stability; alpha1 not sig
fit10s7	ar1,2,6,14,16,23,24, and ma1	**-3.299**	AIC= -3.299; otherwise no real improvement in stats
fit10s8	ar1,2,6,14,15,16,23,24 and ma1	**-3.3**	AIC= -3.3; alpha1 sig to 80%;
fit10s9	ar1,2,5,6,14,15,16,23,24 and ma1	**-3.3**	No improvement
fit10s10	ar1,2,6,14,15,16,23, and ma1	**-3.3**	No improvement
fit10s11	ar1,2,6,14,15,16,23,24,48,72,96	**-3.379**	AIC= -3.379; alpha1 not sig; now we have several unstable params
fit10s12	ar1,2,6,14,15,16,24, ma1,2	**-3.14**	AIC= -3.14; poor sig alpha1, ar16, ma2
fit10s8a	ar1,2,6,14,15,16,23, and ma1	**-3.35**	AIC= -3.35, ar23 still problematic
fit10s8b	ar1,2,6,14,15,16, and ma1	**-3.22**	AIC=-3.22; alpha 1 not very sig; correlation of residuals excellent

Progression of Models - Winter		
Model ID	**Fixed parameter models**	**AIC**
fit1w	eGARCH(2,1) ARMA(24,1) sstd reg	-3.63
fit2w	ar1,2,6,7,12,14,15,16,17,18, and ma1 with eGARCH(1,1)	
fit3w	ar1,2,6,14,15,16,17,18, and ma1	-3.33
fit4w	ar1,2,6,15,16,17, and ma1	
fit5w	ar1,2,6,16,17, and ma1	-3.3
fit6w	ar1,2,6,17, and ma1	
fit7w	ar1,2,6,24, and ma1	-3.51

Table 4 - Summary of forecast test specifications and results

Forecast tests - year 5					MSE	MAE	DAT
fit10s8	n.ahead=1	n.roll=2399	lndiffsummer	nnsummer5	0.004149	0.046165	1
fit10s4	n.ahead=1	n.roll=2399	lndiffsummer	nnsummer5	0.004294	0.047049	1
fit10s	n.ahead=1	n.roll=2399	lndiffsummer	nnsummer5	0.004078	0.045605	1
fit1w	n.ahead=1	n.roll=4379	lndiffwinter	nnwinter5	0.006151	0.043697	1
fit7w	n.ahead=1	n.roll=4379	lndiffwinter	nnwinter5	0.006860	0.046376	1

Table 5 - Results from selected model specifications and corresponding fit diagnostics

GARCH	eGARCH(2,1)				10s1	eGARCH(1,1)				10s4	eGARCH(1,1)				10s8	eGARCH(1,1)				10s8b
Mean	ARMA(48,1)					ARMA(24,1)					ARMA(24,1)					ARMA(24,1)				
Dist	sstd					sstd					sstd					sstd				
Regressors	xternal reg: max wind/max load					xternal reg: max wind/max load					xternal reg: max wind/max load					xternal reg: max wind/max load				
Data Set	Indiffsummer					Indiffsummer					Indiffsummer					Indiffsummer				
Parameters																				
	Estimate	**Std Error**	**t value**	**Pr(>|t|)**		**Estimate**	**Std Error**	**t value**	**Pr(>|t|)**		**Estimate**	**Std Error**	**t value**	**Pr(>|t|)**		**Estimate**	**Std Error**	**t value**	**Pr(>|t|)**	
mu	8.06539	0.0026	3102.113	0		8.065458	0.001241	6500.463	0		8.063739	0.001122	7188.251	0		8.063582	0.001008	7998.172	0	
ar1	0.33642	0.038357	8.77084	0		0.439462	0.011031	39.8402	0		0.470461	0.007673	61.3134	0		1.291207	0.003983	324.1851	0	
ar2	-0.01376	0.023483	-0.58592	0.557927		-0.03681	0.005515	-6.6741	0		-0.05229	0.004579	-11.4205	0		-0.48607	0.003291	-147.712	0	
ar6	0	NA	NA	NA		-0.0755	0.004199	-17.9776	0		-0.0739	0.005816	-12.706	0		-0.11766	0.002768	-42.5123	0	
ar14	0	NA	NA	NA		0	NA	NA	NA		-0.02503	0.005499	-4.5522	0.000005		-0.08452	0.003632	-23.2679	0	
ar15	0	NA	NA	NA		0	NA	NA	NA		-0.02184	0.004898	-4.4586	0.000008		-0.0254	0.002271	-11.1826	0	
ar16	0	NA	NA	NA		0	NA	NA	NA		-0.02523	0.003994	-6.3165	0		-0.00272	0.001548	-1.7564	0.079013	
ar23	0	NA	NA	NA		0	NA	NA	NA		0.138336	0.007027	19.685	0		0	NA	NA	NA	
ar24	0.323496	0.015671	20.64332	0		0.409089	0.009581	42.6973	0		0.30219	0.008649	34.9409	0		0	NA	NA	NA	
ar48	0.224111	0.006656	33.67043	0																
ma1	0.163874	0.036536	4.48532	0.000007		0.099387	0.00864	11.5028	0		0.053851	0.007282	7.3952	0		-0.65578	0.005039	-130.143	0	
omega	-3.37179	0.555154	-6.07362	0		-3.98474	0.254874	-15.6342	0		-3.69274	0.242565	-15.2237	0		-4.21921	0.310326	-13.596	0	
alpha1	-0.03693	0.013468	-2.74182	0.00611		-0.03252	0.014009	-2.3216	0.020257		0.019952	0.013964	1.4288	0.153059		0.031251	0.043326	0.7213	0.470726	
alpha2	0.072945	0.015192	4.8017	0.000002																
beta1	0.523679	0.078221	6.69487	0		0.429816	0.036093	11.9085	0		0.478853	0.033833	14.1532	0		0.364014	0.045439	8.0111	0	
gamma1	0.527371	0.024826	21.24277	0		0.535835	0.024914	21.5072	0		0.565755	0.024019	23.5546	0		0.545066	0.034582	15.7615	0	
gamma2	-0.01774	0.058668	-0.30238	0.762362																
vxreg1	1.717445	0.29188	5.88408	0		2.002015	0.150248	13.3248	0		1.877735	0.14493	12.9562	0		1.677838	0.150853	11.1223	0	
skew	0.91524	0.0082	111.6151	0		0.896903	0.007439	120.5655	0		0.916996	0.00779	117.717	0		0.868179	0.008438	102.8936	0	
shape	4.273989	0.140119	30.50257	0		4.164093	0.130771	31.8426	0		4.379142	0.141914	30.8578	0		4.216177	0.15069	27.9792	0	
Log Likelihood	39777.38					39177.93					39787.56					35594.47				
AIC	-3.3005					-3.251					-3.3					-3.22				
Q-stats on Standard Residuals																				
	Q Stat	**p-value**				**Q Stat**	**p-value**				**Q Stat**	**p-value**				**Q Stat**	**p-value**			
Lag[1]	0.1956	0.6583				2.344	0.1258				1.666	0.1968				4.701	0.03014			
Lag[p+q+1][26]	980.9653	0				990.49	0				462.064	0				1333.458	0			
Lag[p+q+5][30]	985.0843	0				1029.682	0				511.148	0				1421.549	0			
d.o.f=2																				
Ho: No serial correlation																				
Q-stats on Squared Residuals																				
Lag[1]	1.63E-05	0.9968				3.16E-05	0.9955				0.000552	0.9813				0.001015	0.9746			
Lag[p+q+1][4]	0.00436	0.9474				0.00268	0.9587				0.002595	0.9594				0.002879	0.9572			
Lag[p+q+5][8]	0.01027	1				0.1109	0.9998				0.039362	1				0.273425	0.9981			
d.o.f=2																				
ARCH LM Test		**p-value**																		
ARCH lag[2]	0.000548	0.9997				0.00071	0.9996				0.001282	0.9994				0.001824	0.9991			
ARCH lag[5]	0.005857	1				0.004614	1				0.004791	1				0.004191	1			
ARCHlag[10]	0.012582	1				0.114291	1				0.041281	1				0.301302	1			
Nyblom stability test		**5% Critical Value**					**5% Critical Value**					**5% Critical Value**					**5% Critical Value**			
mu	0.1753	> 0.47				0.1098	> 0.47				0.04467	> 0.47				0.2448	> 0.47			
ar1	0.8278					0.4663					0.46366					1.1626				
ar2	0.7067					0.9254					0.63639					2.4304				
ar6						0.9881					0.95098					3.5294				
ar14											0.6205					0.8309				
ar15											0.46778					0.5435				
ar16											0.61625					0.2015				
ar23											7.9611									
ar24	16.6529					22.3167					19.116									
ar48	7.7881																			
ma1	3.5762					2.9032					6.75176					7.4232				
omega	0.4305					0.4808					0.45005					0.3555				
alpha1	1.9778					0.6894					0.65814					0.5209				
alpha2	1.6527																			
beta1	0.5576					0.6241					0.62549					0.4125				
gamma1	0.2595					0.1857					0.23974					0.3883				
gamma2	1.8546																			
vxreg1	0.3338					0.3857					0.37237					0.2557				
skew	0.6112					1.7028					0.80041					0.1922				
shape	0.1906					0.3116					0.17836					0.8611				
Sign Bias Test																				
Sign Bias	0.3061					0.3299					0.3229					0.2742				
Negative Sign Bias	0.8827					0.9588					0.9667					0.6138				
Positive Sign Bias	0.8191					0.8271					0.9938					0.9412				
Joint Effect	0.7425					0.8					0.7636					0.6797				

Sign Bias, testing the null hypothesis that no asymmetry remains in the residuals - * = reject the null with low significance, ** = moderate significance, *** = high significance

Table 6 - Results from selected model specifications and corresponding fit diagnostics

GARCH	eGARCH(1,1)				1w	eGARCH(1,1)				3w	eGARCH(1,1)				5w	eGARCH(1,1)				7w
Mean	ARMA(24,1)					ARMA(24,1)					ARMA(24,1)					ARMA(24,1)				
Dist	sstd					sstd					sstd					sstd				
Regressors	xternal reg: max wind/max load					xternal reg: max wind/max load					xternal reg: max wind/max load					xternal reg: max wind/max load				
Data Set	lndiffwinter					lndiffwinter					lndiffwinter					lndiffwinter				
Parameters																				
	Estimate	**Std. Error**	**t value**		**Pr(>|t|)**	**Estimate**	**Std. Error**	**t value**		**Pr(>|t|)**	**Estimate**	**Std. Error**	**t value**		**Pr(>|t|)**	**Estimate**	**Std. Error**	**t value**		**Pr(>|t|)**
mu	8.26496	0.00451	1834.72269		0	8.26520	0.00104	7956.94805		0	8.26548	0.00143	5791.95880		0	8.26512	0.00135	6136.73710		0
ar1	0.32524	0.03141	10.35352		0	1.24491	0.01747	71.26728		0	1.24853	0.00899	138.87950		0	0.39644	0.01702	23.29390		0
ar2	-0.04672	0.01838	-2.54169		0.011032	-0.52048	0.00950	-54.78791		0	-0.52391	0.00478	-109.52170		0	-0.12316	0.01023	-12.03980		0
ar3	-0.05218	0.00493	-10.57446		0	0.00000	NA	NA	NA		0.00000	NA	NA	NA		0.00000	NA	NA	NA	
ar4	-0.01601	0.00716	-2.23538		0.025392	0.00000	NA	NA	NA		0.00000	NA	NA	NA		0.00000	NA	NA	NA	
ar5	-0.02573	0.00825	-3.12049		0.001805	0.00000	NA	NA	NA		0.00000	NA	NA	NA		0.00000	NA	NA	NA	
ar6	-0.05096	0.00573	-8.89850		0	-0.12261	0.01052	-11.64971		0	-0.09684	0.00279	-34.76480		0	-0.09387	0.00420	-22.37620		0
ar7	-0.04615	0.00446	-10.34266		0	0.00000	NA	NA	NA		0.00000	NA	NA	NA		0.00000	NA	NA	NA	
ar8	-0.07170	0.00552	-12.98597		0	0.00000	NA	NA	NA		0.00000	NA	NA	NA		0.00000	NA	NA	NA	
ar9	-0.03525	0.00725	-4.86405		0.000001	0.00000	NA	NA	NA		0.00000	NA	NA	NA		0.00000	NA	NA	NA	
ar10	0.01804	0.00550	3.28056		0.001036	0.00000	NA	NA	NA		0.00000	NA	NA	NA		0.00000	NA	NA	NA	
ar11	0.00218	0.02225	0.09810		0.921856	0.00000	NA	NA	NA		0.00000	NA	NA	NA		0.00000	NA	NA	NA	
ar12	-0.02877	0.01141	-2.52238		0.011656	0.00000	NA	NA	NA		0.00000	NA	NA	NA		0.00000	NA	NA	NA	
ar13	-0.01333	0.00651	-2.04704		0.040655	0.00000	NA	NA	NA		0.00000	NA	NA	NA		0.00000	NA	NA	NA	
ar14	-0.02216	0.00454	-4.87720		0.000001	-0.03627	0.09094	-0.39885		0.690001	0.00000	NA	NA	NA		0.00000	NA	NA	NA	
ar15	-0.07684	0.00531	-14.46145		0	-0.10031	0.16924	-0.59271		0.553374	0.00000	NA	NA	NA		0.00000	NA	NA	NA	
ar16	-0.05803	0.00518	-11.19958		0	-0.01450	0.00942	-1.53844		0.123942	-0.15385	0.00497	-30.95040		0	0.00000	NA	NA	NA	
ar17	-0.03584	0.00386	-9.29111		0	0.02815	0.15951	0.17649		0.859911	0.04337	0.00525	8.25410		0	0.00000	NA	NA	NA	
ar18	-0.02399	0.00330	-7.26981		0	-0.04835	0.09064	-0.53344		0.593729	0.00000	NA	NA	NA		0.00000	NA	NA	NA	
ar19	-0.00900	0.00313	-2.87711		0.004013	0.00000	NA	NA	NA		0.00000	NA	NA	NA		0.00000	NA	NA	NA	
ar20	-0.02937	0.00387	-7.58399		0	0.00000	NA	NA	NA		0.00000	NA	NA	NA		0.00000	NA	NA	NA	
ar21	-0.04340	0.00463	-9.36537		0	0.00000	NA	NA	NA		0.00000	NA	NA	NA		0.00000	NA	NA	NA	
ar22	-0.05843	0.00593	-9.85083		0	0.00000	NA	NA	NA		0.00000	NA	NA	NA		0.00000	NA	NA	NA	
ar23	0.14919	0.00576	25.89080		0	0.00000	NA	NA	NA		0.00000	NA	NA	NA		0.00000	NA	NA	NA	
ar24	0.37523	0.01861	20.16757		0	0.00000	NA	NA	NA		0.00000	NA	NA	NA		0.53674	0.01198	44.80990		0
ma1	0.29462	0.03837	7.67753		0	-0.55054	0.01870	-29.43483		0	-0.54364	0.01769	-30.73360		0	0.23875	0.01325	18.01520		0
omega	-1.65609	0.51493	-3.21613		0.001299	-2.81362	0.43148	-6.52080		0	-2.66448	0.24759	-10.76170		0	-0.61061	0.04787	-12.75600		0
alpha1	0.06176	0.10582	0.58366		0.559451	0.12766	0.02875	4.44061		0.000009	0.13736	0.03109	4.41840		0.00001	0.05521	0.00816	6.76910		0
beta1	0.77305	0.07031	10.99530		0	0.58321	0.06440	9.05554		0	0.60224	0.03755	16.03970		0	0.91520	0.00667	137.28730		0
gamma1	0.46940	0.03689	12.72370		0	0.45715	0.02973	15.37710		0	0.44601	0.02452	18.19160		0	0.26538	0.03116	8.51790		0
vxreg1	0.80425	0.28259	2.84601		0.004427	1.03064	0.17061	6.04110		0	0.95149	0.10646	8.93750		0	0.30268	0.03031	9.98620		0
skew	0.97318	0.02593	37.53559		0	0.98776	0.01307	75.59946		0	0.99673	0.01069	93.26880		0	0.97123	0.00984	98.66860		0
shape	5.18995	0.43033	12.06032		0	6.12496	0.40912	14.97110		0	6.30346	0.40915	15.40620		0	5.28588	0.24680	21.41810		
Log Likelihood	39471.35					36266.92					35884.76					38197.5				
AIC	-3.63					-3.33					-3.3					-3.51				
Q-stats on Standard Residuals																				
	Q Stat	**p-value**																		
Lag[1]	0.05174	0.8201				1.244	0.2647				1.186	0.2761				0.2559	0.613			
Lag[p+q+1][26]	158.2205	0				462.023	0				908.967	0				346.1798	0			
Lag[p+q+5][30]	161.0503	0				482.706	0				934.098	0				348.1125	0			
d.o.f=2																				
Ho: No serial correlation																				
Q-stats on Squared Residuals																				
Lag[1]	3.53E-05	0.9953				9.98E-05	0.992				0.000113	0.9915				2.46E-05	0.996			
Lag[p+q+1][4]	0.000227	0.988				0.000286	0.9865				0.00033	0.9855				0.000261	0.9871			
Lag[p+q+5][8]	0.000684	1				0.00246	1				0.001564	1				0.000748	1			
d.o.f=2																				
ARCH LM Test		**p-value**																		
ARCH lag[2]	7.94E-05	1				0.000195	0.9999				0.000218	0.9999				0.000102	0.9999			
ARCH lag[5]	0.000506	1				0.000565	1				0.000667	1				0.000559	1			
ARCHlag[10]	0.000937	1				0.002579	1				0.001631	1				0.001069	1			
Nyblom stability test		**5% Critical Value**					**5% Critical Value**					**5% Critical Value**					**5% Critical Value**			
mu	0.07988	> 0.47				0.6571	> 0.47				0.66722	> 0.47				0.05635	> 0.47			
ar1	1.11095					0.113					0.15546					0.79167				
ar2	1.40329					1.4758					1.37081					1.66565				
ar3	1.00087																			
ar4	0.23939																			
ar5	0.56649																			
ar6	0.87125					2.1773					1.30555					0.88849				
ar7	0.75322																			
ar8	0.46424																			
ar9	0.65699																			
ar10	0.05668																			
ar11	0.04249																			
ar12	0.27238																			
ar13	0.17061																			
ar14	0.03807					0.4987														
ar15	0.24897					1.2251														
ar16	0.12615					0.6443					0.56098									
ar17	0.07258					0.163					0.07427									
ar18	0.02474					0.1181														
ar19	0.03485																			
ar20	0.05944																			
ar21	0.05887																			
ar22	0.01903																			
ar23	4.15071																			
ar24	15.04007															18.47509				
ma1	1.62329					0.3163					1.54385					4.37791				
omega	1.15576					1.1665					1.15571					0.79972				
alpha1	1.79752					3.3237					3.66622					2.15562				
beta1	0.80418					1.0076					1.02505					0.57822				
gamma1	1.86549					0.7898					1.02085					2.97351				
vxreg1	1.90548					1.8219					1.78223					1.31965				
skew	0.28224					2.1116					1.89985					0.47843				
shape	0.5363					0.383					0.2424					0.54674				
Sign Bias Test																				
Sign Bias	0.4355					0.3596					0.3539					0.4193				
Negative Sign Bias	0.9837					0.9818					0.9868					0.9821				
Positive Sign Bias	0.6146					0.9893					0.9226					0.6647				
Joint Effect	0.7614					0.8112					0.7898					0.7773				

Sign Bias, testing the null hypothesis that no asymmetry remains in the residuals - * = reject the null with low significance, ** = moderate significance, *** = high significance

Works Cited

Akaike, H. (1998), Information theory and an extension of the maximum likelihood principle, in Selected Papers of Hirotugu Akaike, pp. 199–213, Springer.

Ailliot, P., and V. Monbet (2012), Markov-switching autoregressive models for wind time series, Environmental Modelling & Software, 30, 92–101.

Bauwens, L., C. Hafner, and S. Laurent (2012), Handbook of Volatility Models and Their Applications.

Black, M., and G. Strbac (2007), Value of Bulk Energy Storage for Managing Wind Power Fluctuations, IEEE Transactions on Energy Conversion, 22(1), 197–205, doi:10.1109/TEC.2006.889619.

Bollerslev, T. (1986), Generalized autoregressive conditional heteroskedasticity, Journal of econometrics, 31(3), 307–327.

BPA (2013), BPA revises policy for managing seasonal power oversupply, Available from: http://www.bpa.gov/news/newsroom/pages/BPA-revises-policy-for-managing-seasonal-power-oversupply.aspx (Accessed 22 May 2014).

BPA Wind, WIND GENERATION & Total Load in The BPA Balancing Authority, http://transmission.bpa.gov/Business/Operations/Wind/default.aspx (Accesssed 18 July 2013).

Chen, P., T. Pedersen, B. Bak-Jensen, and Z. Chen (2010), ARIMA-based time series model of stochastic wind power generation, Power Systems, IEEE Transactions on, 25(2), 667–676.

Ela, E., B. Kirby, E. Lannoye, M. Milligan, D. Flynn, B. Zavadil, and M. O'Malley (2010), Evolution of operating reserve determination in wind power integration studies, in 2010 IEEE Power and Energy Society General Meeting, pp. 1–8.

Engle, R. F. (1982), Autoregressive conditional heteroscedasticity with estimates of the variance of United Kingdom inflation, Econometrica: Journal of the Econometric Society, 987–1007.

Engle, R. F., and V. K. Ng (1993), Measuring and testing the impact of news on volatility, The journal of finance, 48(5), 1749–1778.

Farrell, F. E., K. L. Lee, and D. B. Mark (n.d.), Tutorial in Biostatistics, Statistics in Medicine, 15, 361–387.

Foley, A. M., P. G. Leahy, A. Marvuglia, and E. J. McKeogh (2012), Current methods and advances in forecasting of wind power generation, Renewable Energy, 37(1), 1–8.

Ghalanos, A. (2013), [rugarch]: Univariate GARCH Models, R package version 1.2-7, http://cran.r-project.org/web/packages/rugarch/index.html.

Hansen, B. E. (1994), Autoregressive conditional density estimation, International Economic Review, 705–730.

Hipel, K., and A. I. McLeod (2004), Time Series Modelling of Water Resources and Environmental Systems.

Hodge, B., and M. Milligan (2011), Wind power forecasting error distributions over multiple timescales, in Power and Energy Society General Meeting, 2011 IEEE, pp. 1–8, IEEE.

Holttinen, H., M. Milligan, E. Ela, N. Menemenlis, J. Dobschinski, B. Rawn, R. J. Bessa, D. Flynn, E. Gomez Lazaro, and N. Detlefsen (2013), Methodologies to determine operating reserves due to increased wind power, in 2013 IEEE Power and Energy Society General Meeting (PES), pp. 1–10.

Huang, Z., and Z. S. Chalabi (1995), Use of time-series analysis to model and forecast wind speed, Journal of Wind Engineering and Industrial Aerodynamics, 56(2), 311–322.

Jeon, J., and J. W. Taylor (2012), Using Conditional Kernel Density Estimation for Wind Power Density Forecasting, J. Am. Stat. Assoc., 107(497), 66–79, doi:10.1080/01621459.2011.643745.

Jiang, W., Z. Yan, D.-H. Feng, and Z. Hu (2012), Wind speed forecasting using autoregressive moving average/generalized autoregressive conditional heteroscedasticity model, Eur. Trans. Electr. Power, 22(5), 662–673, doi:10.1002/etep.596.

Lau, A., and P. McSharry (2010), Approaches for multi-step density forecasts with application to aggregated wind power, The Annals of Applied Statistics, 4(3), 1311–1341.

Lei, M., L. Shiyan, J. Chuanwen, L. Hongling, and Z. Yan (2009), A review on the forecasting of wind speed and generated power, Renewable and Sustainable Energy Reviews, 13(4), 915–920.

Liu, H., E. Erdem, and J. Shi (2011), Comprehensive evaluation of ARMA–GARCH (-M) approaches for modeling the mean and volatility of wind speed, Applied Energy, 88(3), 724–732.

Liu, P., T. Nguyen, X. Cai, and X. Jiang (2012), Finding Multiple Optimal Solutions to Optimal Load Distribution Problem in Hydropower Plant, Energies (19961073), 5(5), 1413–1432, doi:10.3390/en5051413.

Ljung, G. M., and G. E. P. Box (1978), On a measure of lack of fit in time series models, Biometrika, 65(2), 297–303, doi:10.1093/biomet/65.2.297.

Mauch, B., J. Apt, P. M. S. Carvalho, and P. Jaramillo (2013), What day-ahead reserves are needed in electric grids with high levels of wind power?, Environ. Res. Lett., 8(3), 034013, doi:10.1088/1748-9326/8/3/034013.

Nelson, D. B. (1991), Conditional heteroskedasticity in asset returns: A new approach, Econometrica: Journal of the Econometric Society, 347–370.

Nyblom, J. (1989), Testing for the Constancy of Parameters over Time, Journal of the American Statistical Association, 84(405), 223–230, doi:10.1080/01621459.1989.10478759.

Pinson, P., and H. Madsen (2012), Adaptive modelling and forecasting of offshore wind power fluctuations with Markov-switching autoregressive models, Journal of Forecasting, 31(4), 281–313.

R Core Team (2013), R: A Language and Environment for Statistical Computing, R Foundation for Statistical Computing, Vienna, Austria, http://www.R-project.org.

Sfetsos, A. (2000), A comparison of various forecasting techniques applied to mean hourly wind speed time series, Renewable Energy, 21(1), 23–35.

Soman, S. S., H. Zareipour, O. Malik, and P. Mandal (2010), A review of wind power and wind speed forecasting methods with different time horizons, in North American Power Symposium (NAPS), 2010, pp. 1–8, IEEE.

Sturt, A., and G. Strbac (2011a), A times series model for the aggregate GB wind output circa 2030, in IET Conference on Renewable Power Generation (RPG 2011), pp. 1–6.

Sturt, A., and G. Strbac (2011b), Time series modelling of power output for large-scale wind fleets, Wind Energy, 14(8), 953–966, doi:10.1002/we.459.

Tan, G. (2010), Use of a Stochastic Regression Model GARCH for Wind Fluctuation Study, Int. J. Vent., 9(2), 177–189.

Tol, R. S. J. (1997), Autoregressive Conditional Heteroscedasticity in daily wind speed measurements, Theor Appl Climatol, 56(1-2), 113–122, doi:10.1007/BF00863788.

Trombe, P.-J., P. Pinson, and H. Madsen (2012), A General Probabilistic Forecasting Framework for Offshore Wind Power Fluctuations, Energies, 5(3), 621–657, doi:10.3390/en5030621.

Wang, J., A. Botterud, R. Bessa, H. Keko, L. Carvalho, D. Issicaba, J. Sumaili, and V. Miranda (2011), Wind power forecasting uncertainty and unit commitment, Applied Energy, 88(11), 4014–4023.

White, H. (1982), Maximum likelihood estimation of misspecified models, Econometrica: Jour-

nal of the Econometric Society, 1–25.

Part III

Cost Minimization of Power Generation with Intermittent Resources and Energy Storage

Introduction

Many countries and 30 U.S. states plus the District of Columbia have implemented renewable portfolio standards (RPS) that, combined with federal incentives, are driving investment in wind and solar power [US EIA, 2012]. Even states without RPS have experienced growth in renewable energy production as a result of just the federal incentives. Futhermore, although sensitive to cost, price and policy assumptions, the Annual Energy Outlook 2014 Reference Case projects U.S. renewable electricity generation to increase by 69% by 2040 [Conti et al., 2014]. Perhaps more importantly, wind penetration is targeted by the US Department of Energy to increase to 20% by 2030 [O'Connell and Pletka, 2007] and is on a path to achieve that goal [Wiser and Bolinger, 2014]. At these levels, intermittent energy resources such as wind and solar are creating new challenges for energy system operators. For example, twice in recent years, high wind power output coincided with high spring river flows (and thus hydropower output), creating an oversupply situation for Bonneville Power Administration (BPA) [US EIA, 2011]. Carrasco et al. [2006] concluded that energy-storage systems improve the technical performance and economic viability of wind power, particularly when it exceeds about 10% of the total system energy. Although research proceeds on a variety of fronts including storage technologies such as batteries, fuel cells, and hydrogen conversion, viable energy storage world-wide is currently dominated by pumped-storage hydropower (PSH). Nevertheless, application of energy storage in the U.S. has seen limited application [Denholm et al., 2013].

Quantifying the value of storage remains a significant challenge as the costs and benefits of storage are not well understood [Sioshansi et al., 2012]. There is a need for a general model that represents the actual value of using storage to balance intermittent resources and to arbitrage energy, as well as capture the effect of storage on the energy market. Energy storage studies are largely based on exogenous pricing, historic data, and incomplete methods of studying how wind energy affects the economics of storage. The result is that there is little understanding as to how additional storage entering the power market will affect prices, which adds to the already substantial uncertainty facing PSH developers. To improve on previous studies, the objective of this study is to build an optimization/simulation unit commitment model for scheduling storage operations that incorporates: a) pump/turbine efficiency to model design trade-offs; b) uncertainty

due to intermittent power production (in the form of net load); and c) time-scale decomposition for handling design and operational details on the appropriate time scales and achieving a reasonable level of computational efficiency. The model in this chapter is a static mesoscale optimization that incorporates demand uncertainty and uses simulated demand projections developed in chapter II to calculate optimal storage investments given existing grid conditions. The results provide the PSH design parameters for the simulation in chapter IV.

To achieve this objective, an analytical economic model that describes the economic equilibrium conditions of energy storage taking into account variable generation is developed. The model is used to characterize the cost-minimization problem and describe the net value of shifting energy from one period to another in terms of marginal cost. Additionally, it is demonstrated how use the characteristics of the supply curve and exogenous demand time series to develop policies to take advantage of the variability of wind power resources. A case study is developed using pumped energy storage in the federal hydropower system under BPA's control as a way to mitigate extreme wind fluctuations.

The literature touches on the economics of energy storage and variable energy but not in a comprehensive way. Many models incorporate specific regulatory or market assumptions that limit their applicability. Reuter et al. [2012] set their investment model in Germany/Norway and include investment subsidies that do not exist everywhere. Kim and Powell [2011] make a significantly limiting assumption that the storage facility is small in the economy. Benitez et al. [2008] includes both wind and storage but bases the value of storage on reduction in CO_2 with perfect information. Only recently, general storage sizing and pricing models have begun to emerge [Lamont, 2013; Chao, 2011], but fail to address details such as scheduling uncertainty and the role of variable energy resources [Lamont, 2013; Connolly et al., 2011; Crampes and Moreaux, 2010] or of storage technologies [Ambec and Crampes, 2012; Chao, 2011; Botterud et al., 2005].

The model derives the equilibrium condition of a cost-minimizing energy producer making investment decisions. The model in this chapter combines the long-term attributes of storage and intermittent energy generation in a more general way than previously found in literature. The model extends the analysis originally performed by Crampes and Moreaux [2010], who first examined the intertemporal economic efficiency of pairing bulk storage with thermal generation (but not intermittent generation). Ambec and Crampes [2012] did similar analysis of intermittent generation paired

with thermal generation. Chao [2011] calculated the efficiency conditions of intermittent generation with thermal generation and stochastic, price-dependent load. Lamont [2013] did similar analysis based on minimizing system cost and demonstrated the effect of storage on wholesale price, and this paper adds to his analysis by making certain real-world assumptions about operations policy and examining the inter-temporal effects of changing variance in net load. The model uses a similar framework as in Chao [2012], adding storage technology along with intermittent generation. Conclusions are drawn about efficient investment in storage relative to system generation assets and expected demand.

In Section 2, the power system being modeled and the cost minimization problem is presented. The efficiency conditions and discussion are presented in Section 3. An application of the results, based on the simulated net-load from the GARCH model presented in Chapter II, is presented in Section 4, and Section 5 concludes this chapter. Detailed equations and proofs are in the appendices at the end of this chapter.

Methodology

General Description

Stochastic unit commitment is the process of deploying generation assets to meet expected demand at the lowest cost. The cost minimization model is applied to dynamic unit commitment models, like the one in Chapter IV, as well as static models that minimize costs over time considering the average conditions of the system. In this chapter a static cost minimization model is developed that minimizes the costs of a generic power generation system that includes storage over a set of expected demand states based on net load conditions in the Bonneville Power Administration (BPA) balancing area. It is given that the system is constrained to meet an exogenous power demand. The efficiency conditions derived from this model are used to calculate optimal capital investments as well as the expected value of using storage to shift energy from one demand state to another.

The power generation system is specified as a set of n generation technologies and one storage technology, all under the control of a central system operator. The objective of the system

operator is to meet an exogenous demand, D_t, in each timestep at minimal cost. The capacities of the pump/turbine used for pumped storage hydropower and the storage facility are decision variables, as are levels of storage deployment.

Demand is a stochastic process and accounts for both intermittent power generation and consumer demand, both of which are stochastic quantities. Net load is the quantity used here as demand, and is the difference between consumer demand and wind power generation in the BPA balancing area, as described in the GARCH formulation of Part II. This formulation does not create a clear separation between demand side and supply side economics of the problem, but is reasonable because it is a regulatory constraint on most power supply systems that wind power must be fully utilized when it is available. Thus, wind power production is not a decision variable. Neither consumer demand nor wind power generation are assumed to be price responsive or otherwise correlated with each other. It is a limitation of this approach not to model wind power capacity directly as a decision variable. However, wind power capacity is indirectly modeled by the regression of wind penetration with net load GARCH model, and it was shown that scenarios on forecast values of wind penetration can be generated with the GARCH model of Chapter II.

The mix of generation resources available to meet demand defines the system supply curve based on merit order dispatch. Merit order dispatch refers to the principle that, under economically efficient conditions, generation resources are dispatched in the order of least marginal cost to highest, resulting in an increasing supply curve. The unit cost of power generation is not continuous with increasing production because of the merit order dispatch of generators with costs that are modeled as constant over their operating range and that are significantly different than each other. For simplicity, generation supply is illustrated here as an increasing, concave upwards function of total production, $Q(\bullet)$. Realistically, the curve would not be smooth or continuous, but would contain vertical jumps at the points where expensive peaking power is deployed. These characteristics are evident in the dispatch curves compiled by the U.S. Energy Information Administration, such as the one at U.S. EIA [2012] for example.

Storage as a supply-side quantity requires additional consideration. Given an increasing system supply curve describing conventional generation resources, discharging (that is, generating) from storage serves to increase supply while charging (or pumping, in the case of PSH) serves to decrease it. However, pumping and generating do not shift the supply curve uniformly. Pumping,

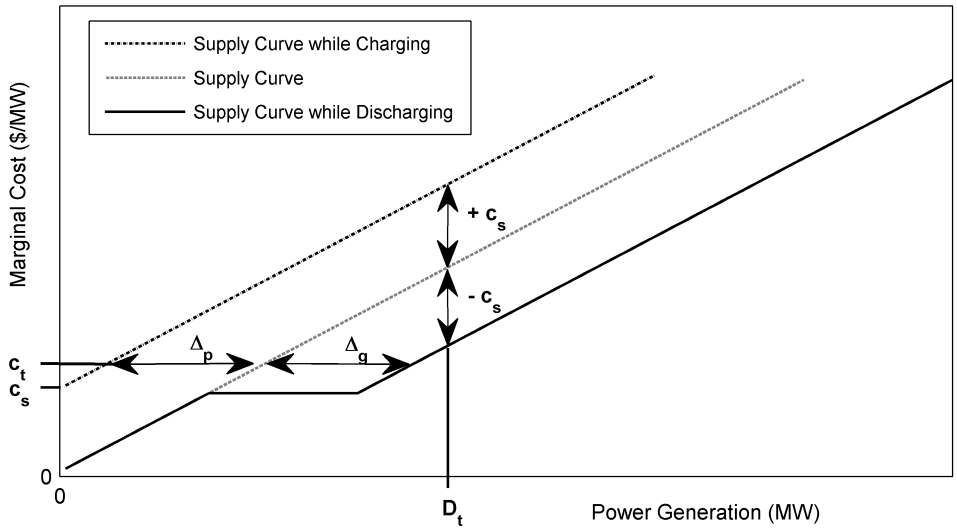

Figure 13: The generation supply curve is shifted to the right, representing an increase in available generation, where generation from storage enters the supply merit order. The entire supply curve is shifted to the left when pumping to storage effectively removes generation from the supply curve and results in an increased marginal price at the origin.

when considered as a supply-side quantity, reduces the supply available to meet demand. The effect is to shift the demand curve inward, or to the left. However, the marginal cost of generating from storage is often lower than the marginal technology, and thus may alter the shape of the supply curve by shifting a portion of the curve such that $c > c_s$ to the right, while leaving the rest unaltered. (See Figure 13.) Correspondingly, the right-hand terminus of the curve is shifted to represent the resulting increase or decrease in available supply to meet demand.

Electricity demand is not consistently price responsive and is modeled here as completely exogenous. Exogenous demand curves are vertical and system marginal cost (SMC) is thus the point on the system curve that intersects $demand = D_t$ (Figure 13). Since energy producers are constrained by regulation to meet that demand, this is a useful approximation. For each time step t a new, vertical demand curve is defined at D_t. The stochastic nature of net load, which is our demand quantity, means that a probability distribution function is defined for each time step for D_t. This stochastic character is used to evaluate the expected value of the cost of generation taking into consideration the time-dependent variance in D_t at each time step using the process described below.

Temporal Context

This expected cost model is calculated at a time scale defined by the length of the storage cycle the storage system is designed for. In this model, the storage cycle is defined to be the time required to fill and then empty the storage reservoir. The hours during the storage cycle used for filling and emptying, respectively, need not be contiguous, but are cumulative within one cycle. The length of the storage cycle is determined by two factors: the power capacity of the pump/turbine and the energy capacity of the storage reservoir. The energy capacity of the reservoir is synonomous with water volume based on the well-defined power function governing the conversion of power to water flow over a vertical displacement. This power function and the selection of power and energy capacity are discussed further below.

Because water reservoirs are costly, they are sized just to meet the energy storage needs of the power system. This energy need defines the characteristic storage cycle based on hours of power discharge. A typical PSH project will have as few as eight hours, and potentially hundreds of hours, of discharge capability. The storage cycle is arrived at by considering the characteristics of the power system - the periodic fluctuations in power price, the available hydrology, and the variability the storage facility is intended to balance.

The system modelled here is heavily dependent on hydropower and experiences small fluctuations in peak-off peak pricing. In the supply curve used in this model, based on production costs publsihed for the Northwest region, the differential between hydropower as the marginal generator and natural gas is approximately 0.38 cents/kw-hr. Relative to other U.S. regions, this is quite small. (See Section for further disucssion.)

Hydropower and natural gas, both of which can be used for peaking power, are very flexible technologies and can alter operating levels on the order of minutes. In that sense, the primary advantages of PSH is the ability of the pump/turbine to reverse modes and consume electricity, its lower cabon footprint compared to natural gas, and the potential efficiency savings compared to natural gas run at partial load. Moreover, hydropower in the BPA system is constrained seasonally by environmental water needs which would not apply to most PSH. Thus, PSH as a peaking generator adds flexibiltiy to the BPA fleet as well as potentially lowering costs.

Considering the seasonal need for flexibiltiy, the strong dependence on hydropower for peaking

power, and the strong daily peaks in both summer and winter (as described in Chapter 2), the PSH developed here operates on a daily cycle. In a daily cycle, PSH located in the BPA system can take advantage of daily low load hour and high load hour pricing. In the optimization step the total energy to be provided by the PSH will be determined.

Determining the minimum cost of the power system at any moment in time is straightforward, but introducing energy storage creates an intertemporal relationship among variables. Given a mix of generation resources and a power demand that defines the state of the system, it is economically efficient to simply dispatch the generators according the merit order. The SMC is then the cost to run the most expensive generator needed to meet demand. When utilizing storage, the constraint that the energy storage must be depleted and recharged on a recurring basis creates the intertemporal dynamic, first described by Crampes and Moreaux [2010]. The intertemporal connection between generating and pumping from PSH is modeled by the constraint that energy stored by pumping must equal energy discharged by generating over the course of a storage cycle. The physical limitation that pumping and generating cannot occur simultaneously is enforced in the mathematical model by the relative costs of pumping and generating and their resulting positions in the merit order: this concept is discussed further below. Under ideal conditions, a storage operator would consider demand and price forecasts and time the filling and discharging of the energy reservoir to minimize system cost. This model averages those decisions over the hours in the storage cycle and a discretized demand probability space, described below.

Assumptions and limitations

Because this is a static, aggregate problem it cannot represent the dynamic properties of power production. Instead, it is intended to provide capacity guidelines given a long-term demand forecast. This aggregation introduces certain assumptions into the problem, particularly as relates to power dispatch dynamics. In this model, the generator fleet is assumed to be fully dispatchable. Planned outages are not explicitly addressed, although capacity values can be scaled to implicitly compensate for maintenance outages. Unscheduled forced outages are neglected. Furthermore, merit order dispatch neglects the various physical limitations of certain generator technologies, such as start up time, minimum run time, and ramping rates.

The additional limiting assumption is made here that the characteristic energy storage cycle is predetermined. A predetermined cycle length may be sub-optimal compared to an optimized cycle length. However, using a predetermined cycle length is a reasonable simplificaiton considering that optimal operation decisions are a practical impossibility because of uncertain forecasts, technical operating constraints that prevent economically efficient dispatch, and concurrent use objectives, such as water supply for environmental services or consumption, that further constrain the operating schedule.

Note that the cost of pumping is the cost of running the pump plus the cost of the marginal generator providing the power to run the pump. Therefore pumping never fits into the merit order dispatch under efficient condtions unless supply exceeds demand. In the absence of over-supply conditions, the purpose of pumping is to balance generating that took place in another period. The problem of over-supply is neglected in the main model formulation and is discussed briefly at the end of the chapter.

It is further assumed that sufficient generation capacity exists to serve demand with 98% reliability, and that storage is fully deployable at all times. Forced outages and tranmission congestion are neglected by this assumption, but are beyond the scope of this model.

Scenario details

In this section the specifics of the mathematical model are outlined in detail. Table 8 provides a rundown of the variables.

Generation Resources

The generation production fleet consists of n generation technologies and one storage technology under the control of a central operator whose objective is to minimize cost and meet an exogenous net demand for power at every hourly time step. Each of the n generators in the fleet has a unit operating cost c_i (\$/MWh), assumed here to be constant over the operating range of the generator. The installed capacity of each generator in the fleet is K_i (MW). Because of the merit order rank based on unit cost, each generator is typically dispatched to its full capacity, K_i, except for the marginal generator denoted $d \in \{1..n\}$, which generates at power level $q_d < K_d$, determined by the

production function $Q_i(D, Z_i)$ defined below.

Energy Storage

Energy storage is treated separately from generation because it must be described both in terms of power capacity as well as energy capacity. PSH is the storage technology of interest for this paper, although it is not the only technology of commercial interest [Eyer and Corey, 2010]. PSH stores energy by pumping water at a flow rate Q (m^3/s) to a reservoir at an elevation H (m), thus converting electrical energy to potential energy. When the water is released downhill, it is converted by the turbine back to electric energy. Both pumping and generating incur efficiency losses of μ_j, where j indicates whether the storage is in pump or generating mode, $j = \{p, g\}$. As a result, power converted to stored energy and back suffers a roundtrip loss of $\mu_p \mu_g = \mu$.

Neither the power capacity fo the pump/turbine (which is the maximum charging rate) nor the energy storage capacity dwarfs the other in terms of capital cost, and are considered separately [EPRI, 1989]. The power capacity of a storage system is the rate of flow of energy that it is capable of achieving. In the case of PSH power capacity is the nameplate capacity of the pump/turbine in MW, K_s, which has a unit capital cost of r_s dollars per megawatt installed ($/MW). The rated power in pumping mode is not necessarily equal to the power rating of the generator. In this model, they are taken to be the same because of the interest in long-term costs of storing energy rather than the detailed operations, although specifying them separately based on manufacturer's information would not make the problem intractable. Pump/generation power, $\bar{\Delta}_j$, is the gridside power quantity consumed/discharged (averaged over feasible operation hours) by the pump/turbine. In the mathematical model, $\bar{\Delta}_j \geq 0$ for both pumping and generating and is defined to be the average power consumption or discharge over the period of feasible operations. Note that the defintion of feasible operations for the pump/turbine in either mode can be variously defined, and is defined for this model below. The unit cost of operating the pump/turbine is denoted c_s ($/MWh). The energy capacity of PSH is the physical volume of the reservoir, which implies the ability to generate power for a time until the reservoir is empty. Energy capacity is denoted K_E MWh at a unit cost of r_E dollars per megawatt-hour of energy ($/MWh).

The total efficiency of a pump/turbine is on the order of 80% to 92%. Efficiency losses can

be significant, particularly when considering that the total efficiency results in the need to pump in excess of scheduled generation by a factor of μ. For this reason the efficiency of the pump is considered separately from the efficiency of the generator. To relate the production of each to the nameplate capacity of the pump/turbine, consider that nameplate capacity describes the useful output of the pump/turbine for its intended use. In the case of generation, useful generation is the gridside output, and thus $K_s = \bar{\Delta}_g$. In the case of pumping, useful output can be described in terms of the quantity of water pumped uphill. Given the general power equation,

$$P = \gamma QH \tag{6}$$

where P is power (MW), H is average head (elevation) over which the water transferred (m), Q is water flow rate (m^3/s), and γ is a constant with units kg m/s^2, then useful pumping power is $K_s = \gamma QH$. The efficiency is then expressed in terms of gridside power and installed capacity by writing the expressions for efficiency in terms of useful power output divided by total power input.

$$\mu_g = \frac{\bar{\Delta}_g}{\gamma QH} \tag{7}$$

$$\mu_p = \frac{\gamma QH}{\bar{\Delta}_p}. \tag{8}$$

This result demonstrates the inverse effect of efficiency in the relationship between energy storage and gridside power output. Rearranging terms, two useful results are obtained. Given that water stored in the reservoir creates a physical constraint that energy stored (pumped) must equal energy discharged (through power generation), we get the result

$$\gamma QHt_g = \frac{1}{\mu_g}\bar{\Delta}_g t_g \tag{9}$$

and

$$\gamma QHt_p = \mu_p \bar{\Delta}_p t_p \tag{10}$$

where t_j, $j \in \{p, g\}$ is the portion of the cycle of t hours that each mode of the pump and turbine

was in operation, and $t_p + t_g \leq t$. Setting the righthand sides of the two equations equal yields

$$\mu \frac{\bar{\Delta}_p}{\bar{\Delta}_g} = \frac{t_g}{t_p}. \tag{11}$$

These results describe the operational interdependencies between power, efficiency and time. For one, the energy discharged in each cycle (from the gridside perspective) will be reduced compared to the power used in pumping by the factor μ. Given that energy is the product of power and time, this increase in pumping energy may come in the form of increased average power consumption compared to generating, increased time pumping compared to time generating, or a combination. In the merit order constrained model, the time to generate and to pump is determined by the demand conditions underwhich it is economic to generate. Power therefore takes an average value over this feasible operating period between zero and full capacity, adjusted for efficiency, such that

$$0 \leq \bar{\Delta}_g \leq K_s \tag{12}$$

and

$$0 \leq \bar{\Delta}_p \leq \mu_p K_s. \tag{13}$$

It is useful to express pumping and generating power in terms of an average over the entire storage cycle rather than just the feasible operaing period. Given that the model developed below is a static representation, a dynamic constraint on pumping and generating that prevents them from operating simultaneously is not required. Instead, the feasible operating period is defined in section [ref] based on merit order and total time constraints which serve to effectively limit the operations so that they are mutually exclusive. For this purpose, average generation output and pumping power consumption are defined in terms of the fraction of the storage cycle during which their operations are feasible.

$$\Delta_g = \begin{cases} \bar{\Delta}_g t_g^{'} & c_s \leq c_i \\ 0 & c_s > c_i \end{cases} \tag{14}$$

$$\Delta_p = \begin{cases} 0 & c_s \leq c_i \\ \bar{\Delta}_p t_p^{'} & c_s > c_i \end{cases}. \tag{15}$$

Given that $\bar{\Delta}_j$ is the average power deployed during the feasible hours and $t_j^{'}$ is the fraction of the storage cycle, t hours, during which operation is allowed, Δ_g is the average power deployed over the entire cycle. In terms of energy, this means

$$\Delta_g t = \bar{\Delta}_g t_g^{'} t = Energy\ Discharged \tag{16}$$

The limits on pump/generator output, equations 12 and 13, and the definition of pump/generator power from equations 14 and 15 combine to describe the physical operating constraints on the pump/turbine. The energy constraints are stated in terms of the power equation (equations 9 and 10).

$$\frac{1}{\mu_g}\Delta_g t = \mu_p \Delta_p t \tag{17}$$

and

$$\frac{1}{\mu_g}\Delta_g t \leq K_E. \tag{18}$$

$K_s$and K_E are decision variables and similarly must be constrained. To establish the maximum size of the reservoir, the power rating of the generator is multiplied by projected time of generation per cycle and converted to volume of water ($Q * time$) using equation 6. The result is

$$K_E = \frac{1}{\mu_g} K_s t_g \tag{19}$$

where $t_g = t * t_g^{'}$ is the maximum amount of time the reservoir can discharge at rated capacity, which from the energy constraint can be calculated to be $t_g = \frac{t}{1/\mu_g + 1}$.

Production Function Assuming merit order dispatch and allowing that the cost of generating from storage, c_s, may be less than the marginal generator, c_d, then the sum of all generation

	Variable	Description	Units
Subscripts	j	specifies pumping or generating mode for the pump/turbine $j \in \{p,g\}$	
	i	specifies which generator in the generation fleet, $i \in \{1...n\}$	
	t	indicates a time-dependent quantity specific to storage cycle $t \in \{1..T\}$	
	d	specifies the marginal generator, given Demand D_t	
Time	t, T	length of storage cycle, number of storage cycles	hours
	t_j'	fraction of total time during the storage cycle when the pump/turbine is operational	
	t_j	ideal total time the pump/turbine is operational	hours
Generation	n	number of generation technologies in the generation fleet	
	c_i	unit cost of operating generator i	\$/MWh
	K_i	installed capacity of generator i	MW
	q_d	average power output of marginal generator d	MW
Energy	K_E	installed storage (reservoir) capacity	MWh
	γ	specific gravity of water	
	Q, H	time rate of flow of water, water head on the pump/turbine	cms, m
	r_E	unit capital cost of energy storage (reservoir)	\$/MWh
Storage	K_s	installed pump/storage capacity	MW
	Δ_j	grid-side power consumed/discharged by the pump/turbine, averaged over the storage cycle	MW
	$\bar{\Delta}_j$	grid-side power consumed/discharged by the pump/turbine, averaged over feasible hours	MW
	c_s	unit cost of operating the pump/turbine in either mode	\$/MWh
	μ, μ_j	overall storage cycle efficiency, efficiency of the pump/turbine separately	
	r_s	unit capital cost of the pump/turbine	\$/MW
Cost	C_t	total operating cost in storage cycle $t \in \{1..T\}$	\$
Production	Q_i	total power produced by generators $[1..i]$, plus storage functions	MW
	D_t	(stocastic) demand quantity in storage cycle $t \in \{1..T\}$	MW

Table 8: Summary of notation used in the cost minimization

capacity up to generator i for all $i \in \{1..n\}$ plus the storage operations is

$$Z_i = \sum_{j=0}^{i} K_j - \Delta_p + \Delta_g, \tag{20}$$

$\{Z_i\}$ for all $i \in \{1,...,n\}$ is a complete description of the supply curve given the possible dispatch of pumping power or generating power. Note that the value of Δ_g is constrained to be $0 \leq \Delta_g \leq K_s$, and its value is determined in the optimization based on the absolute value of c_d and the length of time it is operated. Z_i is taken to be the average over the storage cycle, which becomes important in the calculation of energy production in equation 21 below.

The quantity of power produced is a function of demand as well as the generators dispatched since production is constrained to meet demand. Using the notation for Z_i, the production function $Q_i(D_t, Z_i)$ is the total amount of power produced by generators $1..i$ for $i \in \{1..n\}$.

$$Q_i(D_t, Z_i) = min(D_t, Z_i) = min\left(D_t, \left[\sum_{j=0}^{i} K_j + \Delta_g - \Delta_p\right]\right) \tag{21}$$

The marginal generator is the generator d that is dispatched last to meet demand D_t. Based on the definition of Q_i and subscripting the marginal generator with subscript d, the demand quantity will lie between two values of Z_i such that $Z_{d-1} < D \leq Z_d$.

$$Q_d(D_t, Z_d) = D_t = min\left(D_t, \left[\sum_{j=1}^{d} K_j + \Delta_g - \Delta_p\right]\right) \tag{22}$$

To represent the quantity of power deployed by the marginal generator, we define

$$q_d = Z_d - D_t = \sum_{j=1}^{d-1} K_j + \Delta_g - \Delta_p - D_t. \tag{23}$$

The use of the min function to define Q_i causes the function to truncate at the value of D_t, regardless of which generator is marginal. Thus in any cost function that is a function of D_t, total power produced can be specified in terms of $Q_n(D_t, Z_n) = min(D_t, Z_n)$ without loss of generality. In this definition, the origin of the supply curve must be specified in terms of K_0. Here, $K_0 = 0$, such that, when the first generator is the marginal generator, $D_t < K_1$, $q_d = \Delta_g - \Delta_p - D_t$, and $Q_1 = q_d$. Q_0 follows from equation 21. Note that K_0 does not represent a generator and is not included in the

set of all generators, $i = \{1..n\}$, but is a mathematical definition of the origin of the supply curve required for the following result.

Referring to equation 21 and 23, it can be seen that the quantity of power produced by any one generator i is the quantity

$$Q_i - Q_{i-1} = \begin{cases} K_i & Z_i \leq D_t \\ q_i & Z_{i-1} < D_t \leq Z_i \\ 0 & D_t \geq Z_i \end{cases} \tag{24}$$

The operating cost of meeting power demand D_t can then be written as unit cost of energy times the output of each of the generators and the pump/turbine:

$$C_t(D_t) = t\left(\sum_{i=1}^{n} c_i(Q_i - Q_{i-1}) + c_s(\Delta_g + \Delta_p)\right) \tag{25}$$

Demand as a Stochastic Process Demand D_t is a stochastic process that does not depend on any of the production variables. Therefore, the expected cost, C_t, of producing $Q_n(D_t, Z_n)$ is the cost of operating the necessary generators multiplied by the expected value of Q_n and can be written as

$$E[C_t(D_t)] = E\left[t\left(\sum_{i=1}^{n} c_i(Q_i - Q_{i-1}) + c_s(\Delta_g + \Delta_p)\right)\right] \tag{26}$$

where $E[\bullet]$ is the expectation operator.

Net load is simulated from the GARCH model developed in Chapter II on an hourly basis following the procedure in Chapter II. A daily storage cycle has been adopted based on the observed periodicity of net load and a secondary objective of keeping the storage reservoir as small as possible while providing peaking flexibility to the hydropower fleet. To capture the effect of the large change in variance in the net load process from day to day, the conditional variances of the GARCH model, σ_t^2, conditioned on hourly data, are aggregated into daily values by taking the sum of the intra-daily residuals, r_i^2, following the procedure described in Andersen and Bollerslev [1998].

$$\sigma_t^2 = \sum_{i=1}^{k} r_i^2 \tag{27}$$

over the $k = 24$ intra-daily time periods in one cycle. The innovations of the original model were conditioned on the skewed Student's t distribution developed by Hansen [1994] and this conditional distribution is assumed to hold in the aggregate. The quantile distribution function of D_t is defined on the aggregate variance (equation 27) and mean of the stochastic net load process over the period of one storage cycle and discretized on the values of Z_i, the individual generator capacities. The quantiles are defined based on the generator capacities so that the discontinuities in the supply curve do not affect the mean value of D defined on the intervals of the demand quantile function. The value of D_t on the interval (Z_{i-1}, Z_i) is taken to be the expected value over the interval. The quantile function is truncated at [0.01, 0.99], a conservative approach compared to typical reliability standards that stipulate that reserves must be available to ensure 95% reliability [Crow, 2008].

Given this definition of the quantile function, the expectation operator can be understood in terms of the probability of each generator being the marginal generator, and summing over all possibly values of d. Substituting the marginal generator designated by subscript $d \in \{1..i\}$, then the expectation value can understood by writing the cost as being conditional on $Z_{d-1} < D_t \leq Z_d$.

$$E[C_t(D_t)] = \sum_{d=1}^{n} \left[t \left((\sum_{i=1}^{d} c(Q_i - Q_{i-1}) + c_s(\Delta_g + \Delta_p) \mid (Z_{d-1} < D_t \leq Z_d) \right) * Pr(Z_{d-1} < D_t \leq Z_d) \right]. \tag{28}$$

This single-period cost function is the basis of the total cost function, which includes unit capacity costs, that is the objective function of the minimization developed below.

Cost Minimization Problem

a. Cost function

The single-cycle expected cost of power production is expressed by equation 26. Total cost is the sum of single period costs over all cycles plus capacity costs.

$$E[C_t(D_t)] = \sum_{t=1}^{T} E\left[t\left(\sum_{i=1}^{n} c_i(Q_i - Q_{i-1}) + c_s(\Delta_g + \Delta_p)\right)\right]^{(t)} + r_s K_s + r_E K_E, \tag{29}$$

where the superscript $t \in \{1,...,T\}$ designates the individual cycle among T total cycles. The minimum cost is arrived at, given generator capacities, K_i, by selecting storage capacities, K_S and K_E, as well as storage operations in each cycle, $\Delta_g^{(t)}$ and $\Delta_p^{(t)}$.

The physical and operating constraints for each technology were described in detail above, and are summarized in Table 9. The equality constraints allow for substitutions that reduce to overall number of constraints that must be included in the objective function. The equality relationship between the capacity of the pump/turbine and the size of the reservoir combined with the equality constraint between the energy stored and energy discharged in any given cycle allow the elimination of the upper bound on Δ_p and the lower bounds on Δ_g and K_E, as well as the single-cycle storage constraint (equation 18).

Using the superscript (t) to represent single-cycle values and expressing the series of pump/generation decisions as a sum, the resulting optimization problem is therefore

$$\min_{K_s, K_E, \{\Delta_g^{(t)}, \Delta_p^{(t)}\}} E[C_t(D_t)] = \tag{30}$$

$$\min_{K_s, K_E} \sum_{t=1}^{T} \min_{\Delta_g, \Delta_p} E\left[t\left(\sum_{i=1}^{n} c_i(Q_i - Q_{i-1}) + c_s(\Delta_g + \Delta_p)\right)\right]^{(t)} + r_s K_s + r_E K_E$$

subject to

$$\tfrac{1}{\mu_g}\Delta_g t = \mu_p \Delta_p t$$

$$K_E = \frac{1}{\mu_g} K_s t_g,$$

$$\Delta_g / t_g^{'} \leq K_s,$$

$$0 \leq \Delta_p / t_p^{'},$$

Constraint		Description
Eq. 12	$0 \leq \frac{\Delta_g}{t_g'} \leq K_s$	Generating power must be positive and cannot exceed the nameplate capacity of the pump/turbine
Eq. 13	$0 \leq \frac{\Delta_p}{t_p'} \leq \mu_p K_p$	Pumping power must be positive and cannot exceed the nameplate capacity of the pump/turbine, adjusted for efficiency
Eq. 17	$\frac{1}{\mu_g}\Delta_g t = \mu_p \Delta_p t$	Total energy stored must equal energy discharged within the same cycle
Eq. 18	$\frac{1}{\mu_g}\Delta_g t \leq K_E$	Total energy stored in one cycle cannot exceed the capacity of the reservoir
Eq. 19	$K_E = \frac{1}{\mu_g} K_s t_g$	The pump turbine must be sized to fill the reservoir within one storage cycle
	$0 \leq K_s$	Capacity of the pump/turbine must be non-negative
	$0 \leq K_E$	Capacity of the reservoir must be non-negative

Table 9: Summary of operational and physical constraints

and

$$0 \leq K_s.$$

This set of equations is formalized into an optimization problem in the following sections.

b. First order optimality conditions

To calculate the minimum of the cost function, the objective function (eq. 30) and the constraints are combined below to form an augmented cost function, $l(\bar{x}, \bar{\lambda})$, and the necessary conditions for a minimum solution, specifically the Karuhn-Kush-Tucker (KKT) condtions for sationarity and feasibility, must be confirmed. Note that the constraints from eq. 30 have been rewritten so that $0 \leq h(x)$ and the right-hand quantity is multiplied by a unique KKT multiplier and subtracted from the cost function to form the augmented cost function.

$$l(\bar{x}, \bar{\lambda}) = \sum_{t=1}^{T} E\left[t\left(\sum_{i=1}^{n} c_i(Q_i - Q_{i-1}) + c_s(\Delta_g + \Delta_p)\right)\right]^{(t)} + r_s K_s + r_E K_E \tag{31}$$

$$- \sum_{t=1}^{T} \xi_1^{(t)} E[\mu \Delta_p^{(t)} - \Delta_g^{(t)}]$$

$$-\xi_2(K_E - \frac{1}{\mu_g}K_s t_g)$$

$$-\sum_{t=1}^{T}\gamma_g^{(t)}E[K_S - \Delta_g^{(t)}/t_g^{'}]$$

$$-\sum_{t=1}^{T}\lambda_p^{(t)}E[\Delta_p^{(t)}/t_p^{'}]$$

$$-\lambda_s K_s$$

where $\bar{x}$ is defined to be the vector of decision variables and $\bar{\lambda}$ represents the vector of KKT multipliers introduced in the augmented cost function, $\bar{\lambda} = \{\xi_1^{(t)}, \xi_2, \gamma_g^{(t)}, \lambda_p^{(t)}, \lambda_s\}$. (See Table 8.)

The KKT conditions apply to nonlinear functions that are differentiable at the stationary point $\bar{x}*$ such that $\nabla l(\bar{x}*, \bar{\lambda}*) = 0$ on the feasible domain. x* is a local minimum if the necessary conditions are met. The necessary conditions describe the conditions underwhich $\bar{x}*$ could be a minimum, the first being that the gradient of the augmented cost function equals zero. Additionally, the point x* must be feasible - that is, x* must satisfy each of the constraints, the KKT multipliers on the equality constraints must be greater than or equal to zero, and the complementary slackness condition is met. Formally, the KKT conditions are denoted in the offset below.

Karush-Khun-Tucker Necessary Conditions $f(x) = E[C(D_t)]$

$g_i(\bar{x})$is the set of inequality constraints such that $0 \leq g_i(\bar{x})$

$h_j(\bar{x})$is the set of equality constraints such that $0 = h_j(\bar{x})$ (See table 9.)

$l(\bar{x}, \bar{\lambda}) = f(\bar{x}) - \lambda(g_i(\bar{x}) + h_j(\bar{x}))$

Stationarity

$\nabla l(\bar{x}*, \bar{\lambda}*) = 0$

Primal Feasibility

$0 \leq g_i(\bar{x})$

$0 = h_j(\bar{x})$

Dual Feasibility

$\lambda_i \geq 0$ referring to the KKT multipliers on all inequality constraints

Complementary Slackness

$\lambda_i g_i(\bar{x}) = 0$ for all inequality constraints

Combined with certain regularity conditions and second order conditions the point can be confirmed to be a minimum value of the function. The constraints are linear, which is the most restrictive of the regularity (constraint) conditions. This fact, along with the fact that the cost function is linear in each of the decision variables, satisfies the second order condition that the original cost function be convex. The feasible region has a well-defined lower bound, so if a feasible solution exists it will be a global minimum of the cost function. The derivatives of the augmented cost function are detailed in the attached Appendix A.

Results

Economic efficiency conditions

Pumping and Generating The efficiency conditions for Δ_g and Δ_p for a single cycle are determined by setting the derivatives of the augmented cost function to zero.

$$E[t(c_d - c_s)] = E[\xi_1 + \gamma_g / t_g^{'}] \tag{32}$$

$$E[t(c_s + c_d)] = E[\xi_1 \mu_p + \lambda_p / t_p^{'}]. \tag{33}$$

Equation 32 gives the conditions under which generating is economically efficient. On the left hand side of the equation, $c_s \leq c_d$ implies that generation from storage falls within the merit order and results in a positive value. According to the KKT conditions, γ_g is constrained to be non-negative at a minumum solution, and will be greater than zero when $\Delta_g / t_g^{'}$ is equal to K_s, that is, when generation is utilized to its maximum extent. The result is that, when generation is dispatched, ξ_1 is the difference between $(t(c_d - c_s)$ and $\gamma_g / t_g^{'}$. Clearly, when generation is not dispatched to capacity, ξ_1 must be positive, but otherwise may be negative if$\gamma_g / t_g^{'} \geq t(c_d - c_s)$. The multiplier γ_g is the shadow value of additional generating capacity with respect to the pump/turbine. ξ_1 is the shadow value of additional generating when constrained by the quantity of energy stored. Positive γ_g and ξ_1 both imply that additional generating capacity would decrease the overall marginal cost if it were available. When $c_d - c_s$ is small relative to $\gamma_g / t_g^{'}$, the cost of pumping limits the benefits of additional generation capacity.

$\lambda_p$is the multiplier on the lower pumping constraint with respect to pump/turbine capacity. Because energy stored by pumping must equal energy discharged by generating, $\lambda_p > 0$, true when $\Delta_p = 0$ for the period, implies $\gamma_g = 0$. The cost of pumping $c_s + c_d$ is always positive (neglecting the oversupply condition where c_d is negative) so that when storage is utilized within a period, ξ_1 must be positive. Combining equations 32 and 33 demonstrates the relationship between the cost of pumping and the benefit of generating.

$$t\,(E[c_d - c_s] - E[c_s + c_d]) = E[\xi_1 (1 - \mu_p) + \gamma_g / t_g^{'} - \lambda_p / t_p^{'}] \tag{34}$$

The righthand side of equation 34 is the net benefit of storage operations - the difference between the marginal benefit of generating and the marginal cost of pumping. When the benefit of generating is small and the RHS is negative, either ξ_1 must be negative or λ_p must be positive, meaning that storage is not employed at all. When the RHS is positive, implying that the net benefit of storage operations is positive for the period, then $\gamma_g/t_g^{'} \geq \xi_1(1-\mu_p)$. If $\gamma_g > 0$, then $\xi_1 > 0$ as well, given the result above.

If $\gamma_g = 0$, then two results are possible: first, Δ_g is dispatched to partial capacity, implying that $\xi_1 \geq 0$ and $\lambda_p = 0$. Thus, ξ_1 is the shadow value of the energy arbitrage opportunity. If $\Delta_g = 0$, $\lambda_p \geq 0$ and ξ_1 reflects the sum of the net marginal benefit of storage operations plus the shadow value of reducing pumping activity, meaning the net marginal benefit of storage operations were not large enough to make pumping efficient. If the marginal cost of generation, c_d, is lower than the cost of generating from storage, it would be costly to generate from storage at any level, and thus $\xi_1 \leq 0$.

Given the merit order definition of the problem stated above and the result that either λ_p or γ_g must be zero in each period, the values of λ_p, γ_g, and ξ_1 can be deduced from equations 32 and 33 when the expected marginal cost is known. This result is utilized in the computation in section [ref].

The derivatives with respect to storage capacity are

$$r_s = \lambda_s - \xi_2 \frac{t_g}{\mu_g} + \sum_{t=1}^{T} \gamma_g^{(t)} \tag{35}$$

$$r_E = \xi_2. \tag{36}$$

The value of new storage is determined by the sum of the marginal shadow values of additional generation capacity and the shadow cost of additional pump/turbine capacity. Note that $\lambda_s > 0$ when K_s is constrained at its lower bound, $K_s = 0$, and thus will only be greater than zero when γ_g is zero in all time periods.

Note that the marginal benefit of operating storage is composed of two types of terms: γ_g and λ_p are shadow costs that make up the value of additional capacity, as seen in equations 35 and 36. Additionally, the ξ_1 terms are the shadow values that determine the value of energy arbitrage.

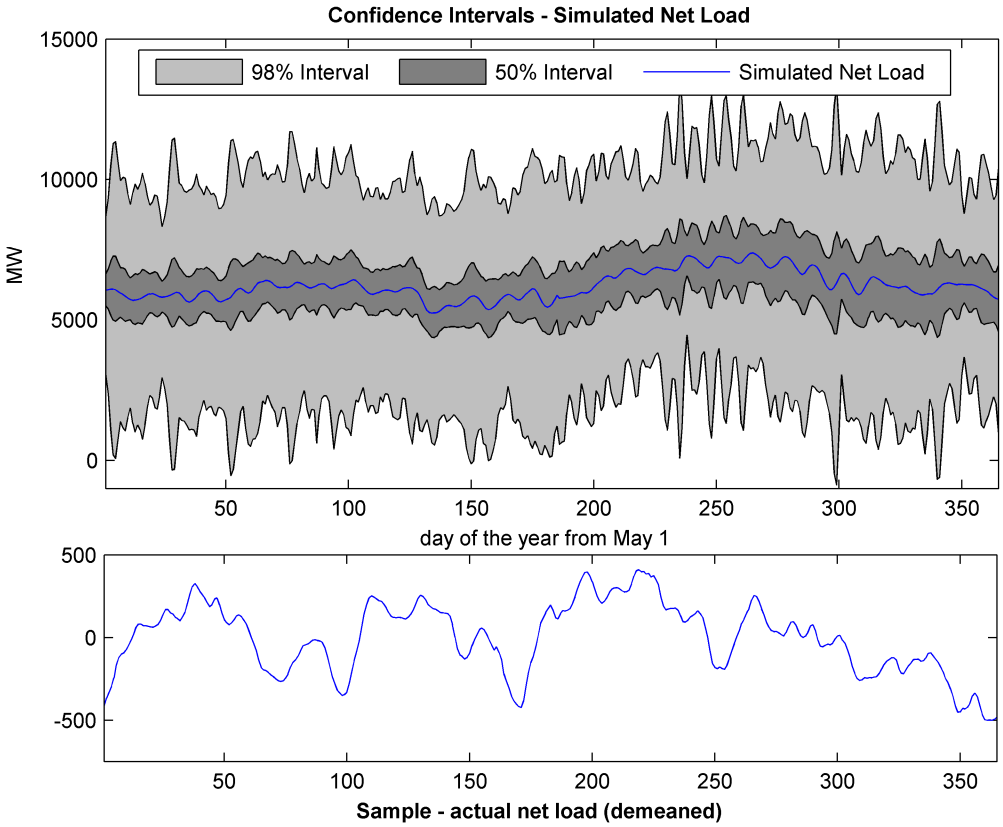

Figure 14: Simulated daily net load scaled to BPA forecasted monthly loads with 98% and 50% confidence intervals. The bottom frame is a sample of the data from which the simulated data was generated for comparison.

Application

Daily net load, aggregated from the hourly simulation data presented in the last chapter, and scaled to forecasted average monthly loads from the 2010 rate case.

Daily observations will follow a weak GARCH process similar to the original hourly model [Andersen and Bollerslev, 1998], and the skewed Student's t distribution from the original model is assumed to hold for these data. Given the capacity values, K_i, for the four generation sectors in Table 10, the probabilities of demand falling between two values of Z_i, and thus the probability of system marginal cost being c_i, are calculated using `rugarch` utilities. The expectation of c_d and therefore the expected costs of using storage are calculated for each period, and equations 32 through 36 provide the framework for determining the shadow values of storage and the value of storage in this system.

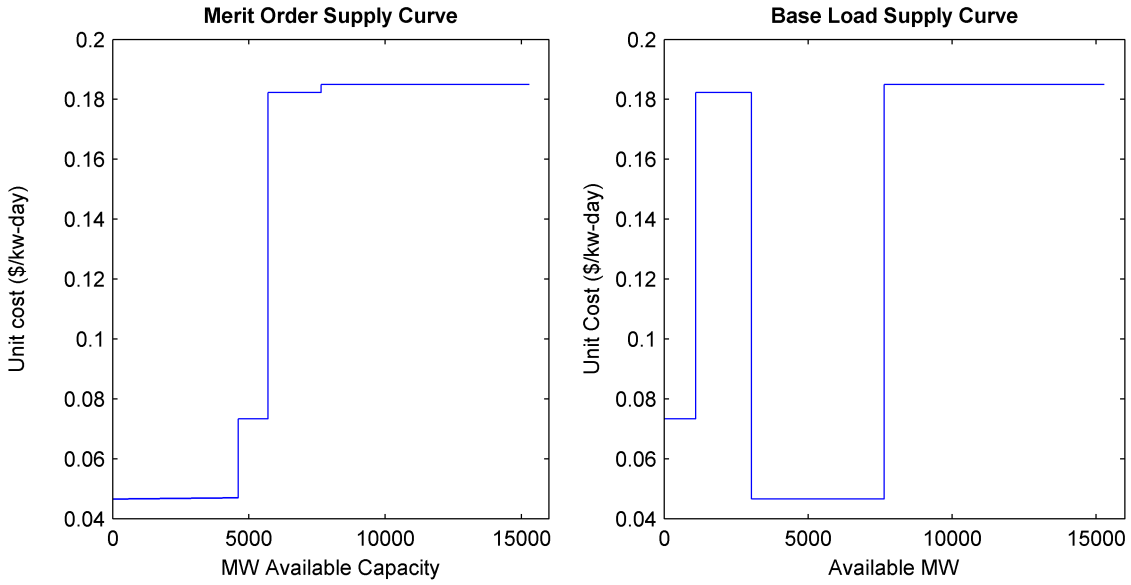

Figure 15: Simplified supply curves used in the model calculation, developed using BPA data. [2010 Rate Case, EIA, 6th Power Plan]

Generator	Merit Order	Unit Operating Cost[3]	Unit Installed Cost
Hydropower	varies monthly[1]	0.047 $/kw-day	3000 $/kW installed
Nuclear	1097 MW[2]	0.073	5500
Coal	1942 MW	0.182	3794
Natural Gas	7635 MW	0.185	1112.5
1. Hydropower is constrained due to water demands at various times of the year. The availablility of hydropower is determined for BPA rate case development based on the 1958 water availability, adjusted for current installed capacity. The monthly estimates used here were adapted from BPA [2010].			
2. Installed capacity in the Northwest as reported in EIA [2010]. No adjustment has been made for forced or planned outages.			
3. Unit costs are adapted from the modeling assumptions of the NWPCC 6th Power Plan [NWPCC, 2012].			

Table 10: Generation parameters used to calculate the conditional probabilities on demand: $Pr(Z_{i-1} < D \leq Z_i)$.

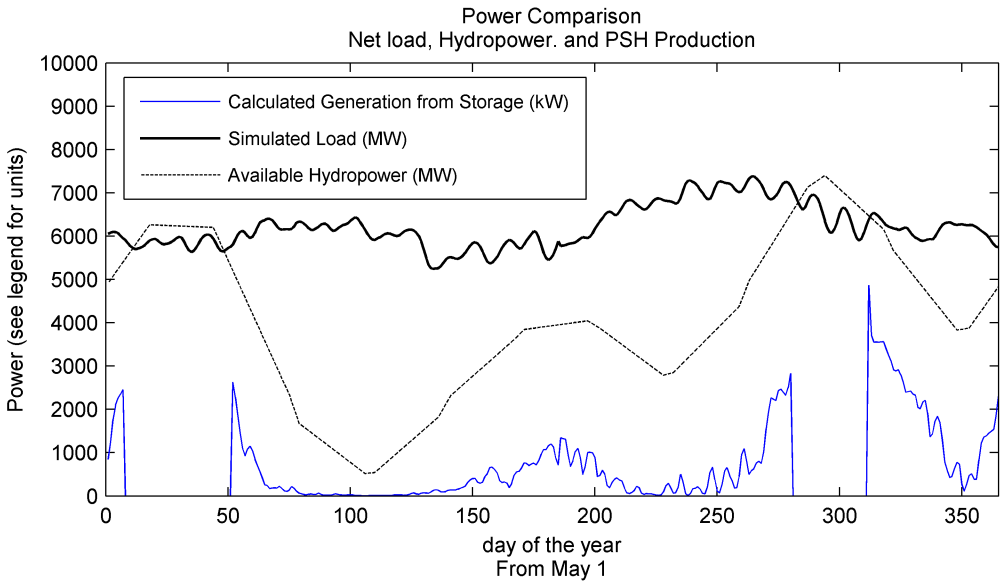

Figure 16: Power quantities over simulation period, assuming 10 MW installed pump/generator capacity.

Multipliers - γ_g is the marginal value of additional capacity available for pumping or generating, which would reduce the cost of power generation. In particular, pump/gen capacity is valuable when the time for either pumping or generating is short. Conversely, ξ_1 is the marginal value of energy arbitrage. The value of arbitrage is affected primarily by the amount of time available for both pumping and generating. A positive value of ξ_1 implies a reduction in marginal cost with an increase in pumping. From Figure it can be seen that arbitrage is most valuable when pumping costs are lowest - that is, when hydropower is plentiful. γ_g and ξ_1 give the complete picture of the potential for obtaining value from pumped storage.

Generation from storage was calculated based on the available time for pumping and storage and an assumed cap of 10 MW of pump/generation capacity. When γ_g is zero, generation Δ_g is likewise zero because it is never economic to deploy PSH at less than full capacity. Given Δ_g, total revenue and total arbitrage value was calculated. Revenue and arbitrage value are often different because a positive net marginal benefit, which translates to revenue, is based on λ_p, γ_g, and ξ_1, such that arbitrage value is less than revenue when the quantity of power arbitraged is limited by capacity. Meanwhile, revenue also depends on the marginal costs within the range of variability of the net load.

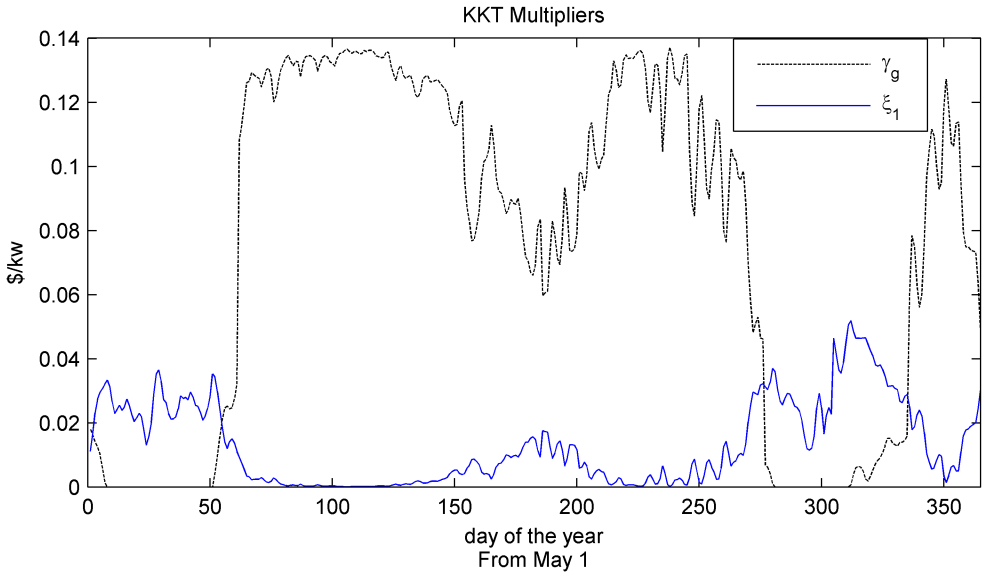

Figure 17: Time series of KKT multipliers associated with energy arbitrage and pump/generator capacity.

Storage Capacity

Given the results from the simulation, the $E[c_s - c_d]$ and $E[c_s + c_d]$ prescribe a shift in the

Appendix A

Augmented Cost Function

$$l(\bar{x},\bar{\lambda}) = \sum_{t=1}^{T} E\left[t\left(\sum_{i=1}^{n} c_i(Q_i - Q_{i-1}) + c_s(\Delta_g + \Delta_p)\right)\right]^{(t)} + r_s K_s + r_E K_E \tag{37}$$

$$-\sum_{t=1}^{T} \xi_1^{(t)} E[\mu\Delta_p^{(t)} - \Delta_g^{(t)}]$$

$$-\xi_2(K_E - \frac{1}{\mu_g} K_s t_g)$$

$$-\sum_{t=1}^{T} \gamma_g^{(t)} E[K_S - \Delta_g^{(t)}/t_g^{'}]$$

$$-\sum_{t=1}^{T} \lambda_p^{(t)} E[\Delta_p^{(t)}/t_p^{'}]$$

$$-\lambda_s K_s$$

Derivatives with respect to short-term decisions: the augmented cost function for each time step (storage cycle) has a set of derivatives given that the quantile function of demand varies with time.

$$\frac{\partial l}{\partial \Delta_g^{(t)}} = E[t(c_s - c_d)] + \xi_1 + \gamma_g/t_g^{'}]$$

$$\frac{\partial l}{\partial \Delta_p^{(t)}} = E\left[t(c_s + c_d) - \xi_1\mu_p - \lambda_p/t_p^{'}\right]^{(t)}$$

Derivatives with respect to long-term decisions: two derivatives of the augmented cost function exist based on pump/turbine and reservoir capacity

$$\frac{\partial l}{\partial K_E} = r_E - \xi_2$$

$$\frac{\partial l}{\partial K_s} = r_s - \lambda_s + \xi_2 \frac{t_g}{\mu_g} - \sum_{t=1}^{T} \gamma_g^{(t)}$$

Derivatives with respect to Lagrange multipliers: derivatives of the augmented cost function exist for each time step for the multipliers $\xi_1^{(t)}$, $\gamma_g^{(t)}$, and $\lambda_p^{(t)}$, along with multipliers that apply to long term conditions, ξ_2 and λ_s.

$$\frac{\partial l}{\partial \xi_1^{(t)}} = -E\left[\mu_p \Delta_p^{(t)} - \Delta_g^{(t)}\right]$$

$$\frac{\partial l}{\partial \gamma^{(t)}} = -E\left[K_s - \Delta_g^{(t)} / t_g^{'}\right]$$

$$\frac{\partial l}{\partial \lambda_p^{(t)}} = -E\left[\Delta_p^{(t)} / t_p^{'}\right]$$

$$\frac{\partial l}{\partial \xi_2} = -\left[K_E - \frac{1}{\mu_g} K_s t_g\right]$$

$$\frac{\partial l}{\partial \lambda_s} = -K_s$$

Works Cited

Ambec, S., and C. Crampes (2012), Electricity provision with intermittent sources of energy, Resource and Energy Economics, 34(3), 319–336, doi:10.1016/j.reseneeco.2012.01.001.

Andersen, T. G., and T. Bollerslev (1998), Answering the Skeptics: Yes, Standard Volatility Models Do Provide Accurate Forecasts, Available from: http://public.econ.duke.edu/~boller/Published_Papers/ier_ (Accessed 23 March 2015)

Benitez, L. E., P. C. Benitez, and G. C. van Kooten (2008), The economics of wind power with energy storage, Energy Economics, 30(4), 1973–1989, doi:10.1016/j.eneco.2007.01.017.

Botterud, A., M. D. Ilic, and I. Wangensteen (2005), Optimal investments in power generation under centralized and decentralized decision making, IEEE Transactions on Power Systems, 20(1), 254 – 263, doi:10.1109/TPWRS.2004.841217.

Carrasco, J. M., L. G. Franquelo, J. T. Bialasiewicz, E. Galvan, R. C. PortilloGuisado, M. A. M. Prats, J. I. Leon, and N. Moreno-Alfonso (2006), Power-Electronic Systems for the Grid Integration of Renewable Energy Sources: A Survey, IEEE Transactions on Industrial Electronics, 53(4), 1002–1016, doi:10.1109/TIE.2006.878356.

Chao, H. (2011), Efficient pricing and investment in electricity markets with intermittent resources, Energy Policy, 39(7), 3945–3953, doi:10.1016/j.enpol.2011.01.010.

Connolly, D., H. Lund, P. Finn, B. V. Mathiesen, and M. Leahy (2011), Practical operation strategies for pumped hydroelectric energy storage (PHES) utilising electricity price arbitrage, Energy Policy, 39(7), 4189–4196.

Conti, J., P. Holtberg, and J. Diefenderfer (2014), Annual Energy Outlook 2014 with Projections to 2040,

Crampes, C., and M. Moreaux (2010), Pumped storage and cost saving, Energy economics, 32(2), 325–333.

Crow, S. (2008), A Resource Adequacy Standard For the Northwest, Northwest Power and Conservation Council, Council Document 2008-07, April, 2008. http://www.nwcouncil.org/media/29608/2008_07.p (Accessed April 12, 2014)

Denholm, P., J. Jorgenson, M. Hummon, T. Jenkin, D. Palchak, B. Kirby, O. Ma, and M. O'Malley (2013), The value of energy storage for grid applications, Technical Report number NREL/TP-

6A20-58465.

EPRI (1989), Pumped-Storage Planning and Evaluation Guide, Electric Power Research Institute, 1989, Technical Report GS-6669.
http://www.epri.com/abstracts/Pages/ProductAbstract.aspx?ProductId=GS-6669, Accessed April 12, 2012.

Eyer, J., and G. Corey (2010), Energy storage for the electricity grid: Benefits and market potential assessment guide, Sandia National Laboratories Report, SAND2010-0815, Albuquerque, New Mexico.

Hansen, B. E. (1994), Autoregressive conditional density estimation, International Economic Review, 705–730. Retrieved from http://www.jstor.org/stable/2527081

Kim, J. H., and W. B. Powell (2011), Optimal Energy Commitments with Storage and Intermittent Supply, Operations Research, 59(6), 1347–1360, doi:10.1287/opre.1110.0971.

Lamont, A. D. (2013), Assessing the Economic Value and Optimal Structure of Large-Scale Electricity Storage, IEEE Transactions on Power Systems, 28(2), 911–921, doi:10.1109/TPWRS.2012.2218135.

O'Connell, R., Pletka, R., et al. (2007), 20 Percent Wind Energy Penetration in the United States: A Technical Analysis of the Energy Resource, Overland Park, KS, Black & Veatch.

Reuter, W. H., S. Fuss, J. Szolgayová, and M. Obersteiner (2012), Investment in wind power and pumped storage in a real options model, Renewable and Sustainable Energy Reviews, 16(4), 2242–2248.

Sioshansi, R., P. Denholm, and T. Jenkin (2012), Market and Policy Barriers to Deployment of Energy Storage, Economics of Energy and Environmental Policy, 1(2), doi:http://dx.doi.org/10.5547/2160-5890.1.2.4.

U.S. Energy Information Administration (2012), Electric generator dispatch depends on system demand and the relative cost of operation, TODAY IN ENERGY, 17th August.

Wiser and Bolinger (2014), 2013 Wind Technologies Market Report, Oak Ridge, TN, US Department of Energy.